Speed: 3D sensors, current amplifiers

Cinzia Da Via

Manchester University

Giovanni Anelli, Matthieu Despeisse[1], Pierre Jarron

CERN

Christopher Kenney, Jasmine Hasi,

SLAC

Angela Kok

SINTEF

Sherwood Parker

University of Hawaii

Initial work and calculations with Julie Segal

Wall electrode data with Edith Walckiers, Philips Semiconductors AG

1. now at Ecole Polytechnique Fédérale de Lausanne (EPFL), Institute of Microengineering (IMT), Photovoltaics and thin film electronics laboratory, Neuchatel, Switzerland.

1. **introduction**
2. **history**
3. **factors affecting speed**
4. **generating the signal – Ramo’s theorem**
5. **amplifying the signal – charge and current amplifiers**
6. **trench electrode sensors**
7. **hex-cell sensors**
8. **experimental results**
9. **analysis – constant fraction discrimination**
10. **analysis – fitting with almost-noise-free pulses**
11. **next**

Potential 3D features from preliminary calculations by Julie Segal:

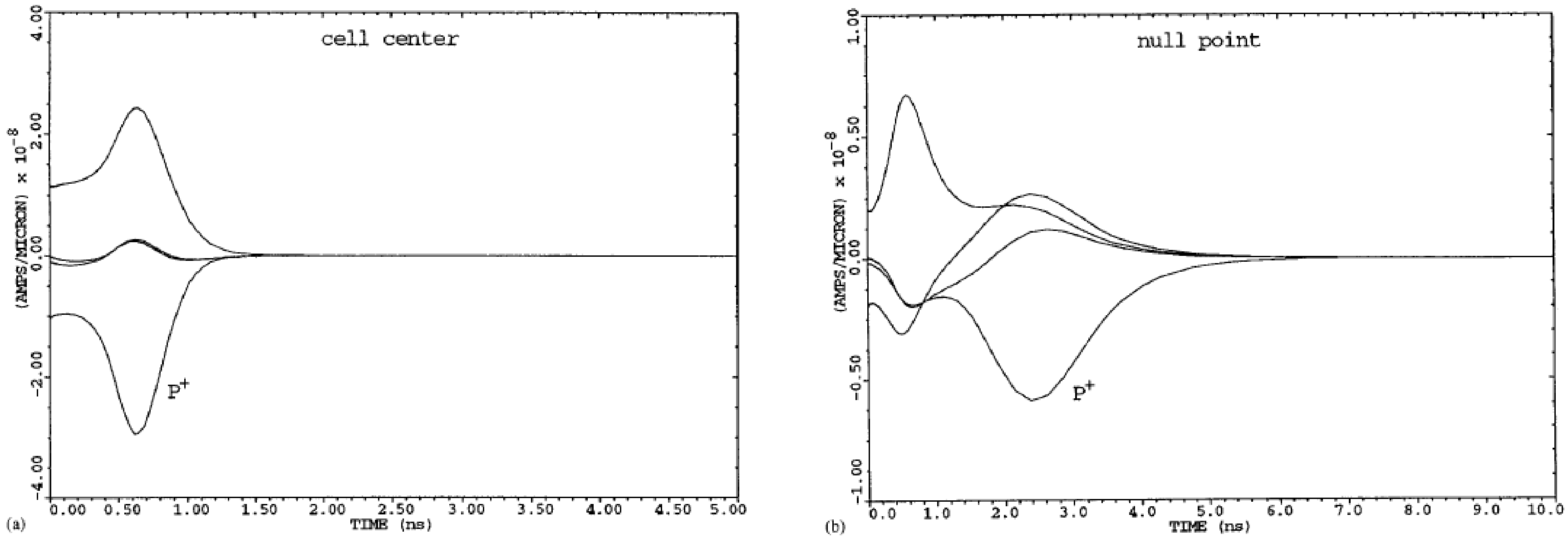

1 ns

3 ns

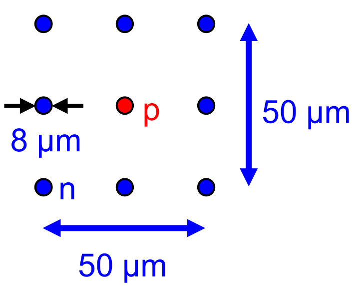

3. Fast pulses. Current to the p electrode and the other 3 n electrodes.

(The track is parallel to the electrodes through a cell center and a null point. V – bias = 10V. Cell centers are in center of any quadrant. Null points are located between pairs of n electrodes.)

Speed: planar → 3D

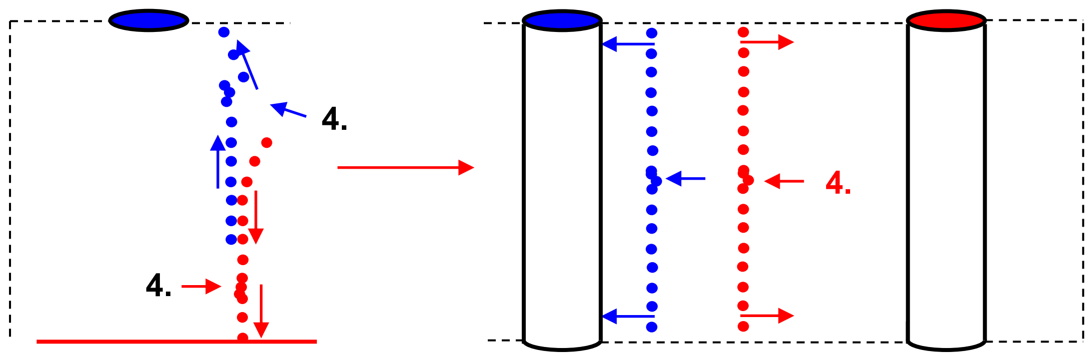

1. 3D lateral cell size can be smaller than wafer thickness, so
2. in 3D, field lines end on electrodes of larger area, so
3. most of the signal is induced when the charge is close to the electrode, where the electrode solid angle is large, so planar signals are spread out in time as the charge arrives, and
4. Landau fluctuations along track arrive sequentially and may cause secondary peaks
5. if readout has inputs from both n+ and p+ electrodes,

1. shorter collection distance
2. higher average fields for any given maximum field (price: larger electrode capacitance)
3. 3D signals are concentrated in time as the track arrives
4. Landau fluctuations (delta ray ionization) arrive nearly simultaneously
5. drift time corrections can be made

1. introduction
2. history
3. factors affecting speed
4. generating the signal – Ramo's theorem
5. amplifying the signal – charge and current amplifiers
6. trench electrode sensors
7. hex-cell sensors
8. experimental results
9. analysis – constant fraction discrimination
10. analysis – fitting with almost-noise-free pulses
11. next

A Very Brief History of Ever Shorter Times

- The first silicon radiation sensors were rather slow with large, high capacitance elements. The resultant noise was reduced by integration.
- For example, in the pioneering UA2 experiment at CERN, "the width of the shaped signal is 2 μs at half amplitude and 4 μs at the base." (Faster discrete-component amplifiers were available, but not widely used.)
- The development of microstrip sensors greatly reduced the capacitance between the top and bottom electrodes, adding a smaller, but significant one between adjacent strips.
- The 128-channel, Microplex VLSI readout chip, had amplifiers with 20 – 25 ns rise times, set by the need to roll off amplification well before
  - $\omega t \leq \pi$ (t = time, input to inverted output then fed back to input)
- (Otherwise we would have produced a chip with 128 oscillators and no amplifiers.)
- The planned use of microstrip detector arrays at colliders with short inter-collision times required a further increase in speed.
- Silicon sensors with 3D electrodes penetrating through the silicon bulk allow charge from long tracks to be collected in a rapid, high-current burst.
- Advanced VLSI technology provides ever higher speed current amplifiers. Up to the sensor speed, such signals grow more rapidly with increasing frequency, than white noise.

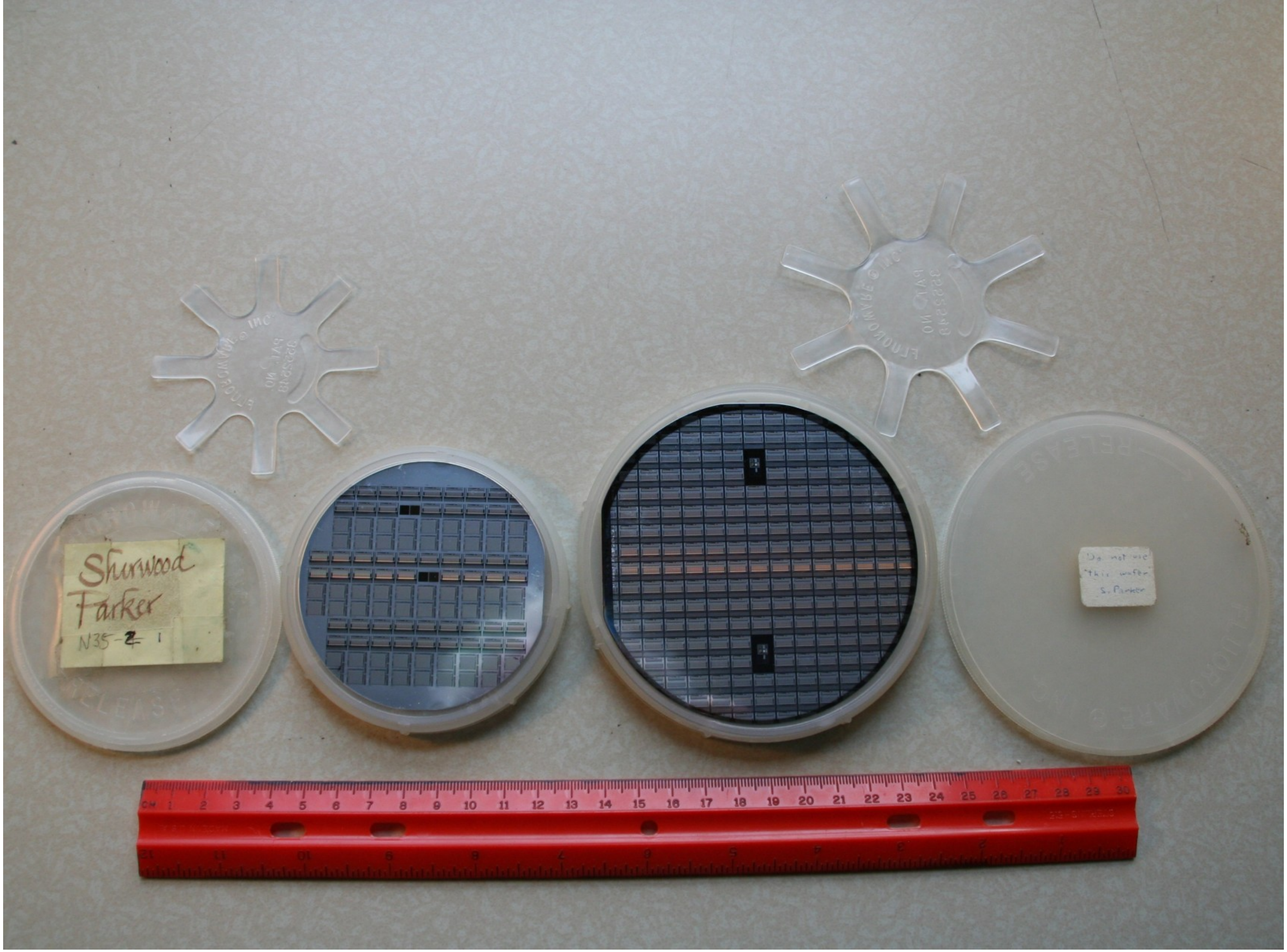

The first ever custom VLSI silicon microstrip readout chips. Made at Stanford in 1984). (left, 7.5 cm), then by AMI – (right, 10 cm).

Nuclear Instruments and Methods in Physics Research A310 (1991) 189–191
North-Holland

NUCLEAR
INSTRUMENTS
& METHODS
IN PHYSICS
RESEARCH
Section A

planar sensor pulse shape

(an early, successful, attempt to increase speed in the era of 1 μs shaping times)

Electrostatic simulations for the design of silicon strip detectors and front-end electronics

R. Sonnenblick, N. Cartiglia, B. Hubbard, J. Leslie, H.F.-W. Sadrozinski and T. Schalk
Santa Cruz Institute for Particle Physics, University of California, Santa Cruz, CA 95064, USA

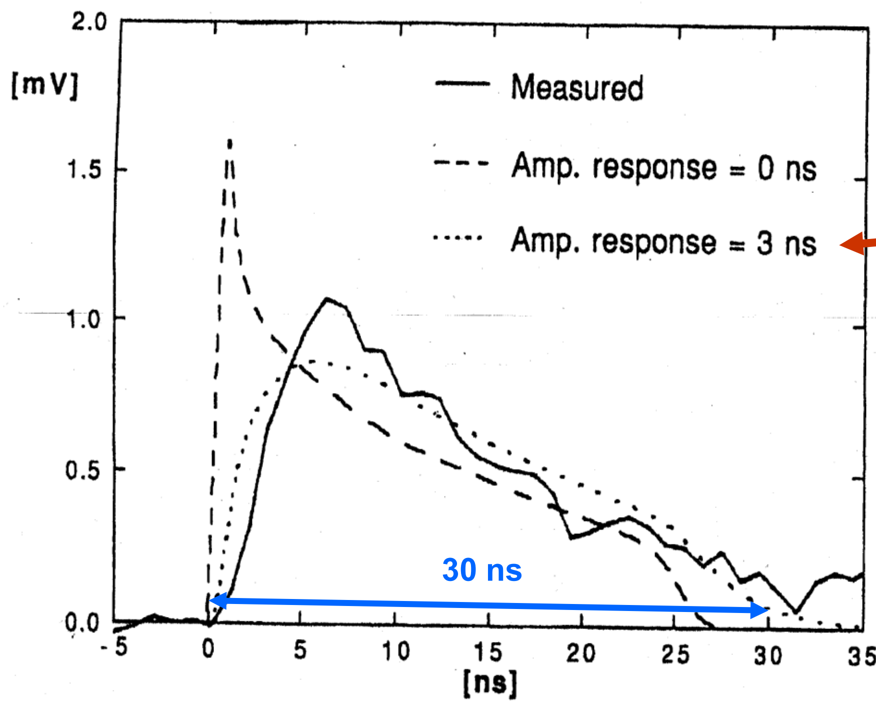

Fig. 3. Pulse shape at the junction side from a minimum ionizing particle. The three curves are the simulated current (with initial diffusion), the simulated current convoluted with the preamplifier response, and a typical observed pulse, respectively.

1. introduction
2. history
3. factors affecting speed
4. generating the signal – Ramo's theorem
5. amplifying the signal – charge and current amplifiers
6. trench electrode sensors
7. hex-cell sensors
8. experimental results
9. analysis – constant fraction discrimination
10. analysis – fitting with almost-noise-free pulses
11. next

Some elements affecting time measurements

1. **variations in track direction** – **1 and 2** can affect the shape and timing of the detected pulse.
2. **variations in track location**
3. **variations in total ionization signal** – can affect the trigger delay.
4. **variations in ionization location along the track** – **Delta rays** – high energy, but still generally non-relativistic, ionization ("knock-on") electrons. Give an ever-larger signal when the Ramo weighting function increases as they approach a planar detector electrode, with their current signal dropping to zero as they are collected. This produces a pulse with a leading edge that has changes of slope which vary from event to event, limiting the accuracy of getting a specific time from a specific signal amplitude for the track.
5. **magnetic field effects affecting charge collection** – E × B forces shift the collection paths but for 3D-barrel only parallel to the track.
6. **measurement errors due to noise** – **This currently is the major error source.**
7. **incomplete use of, or gathering of, available information** – This is a challenge mainly for the data acquisition electronics which, for high speed, will often have to face power and heat removal limitations.
8. In addition, long collection paths for thick planar sensors increase the time needed for readout and decrease the rate capabilities of the system.

1. **introduction**
2. **history**
3. **factors affecting speed**
4. **generating the signal – Ramo's theorem**
5. **amplifying the signal – charge and current amplifiers**
6. **trench electrode sensors**
7. **hex-cell sensors**
8. **experimental results**
9. **analysis – constant fraction discrimination**
10. **analysis – fitting with almost-noise-free pulses**
11. **next**

Calculating the signals

1. **Calculate E fields using a finite element calculation. (Not covered here.)**
2. **Calculate track charge deposition using Landau fluctuating value for (dE/dx) divided by 3.62 eV per hole-electron pair.**
3. **Paths of energetic delta rays may be generated using *Casino,* a program from scanning electron microscopy. (GEANT4 may be used for some of 2 and 3.)**
4. **Calculate velocities and diffusion using C. Jacoboni, et al. "A review of some charge transport properties of silicon" *Solid-State Electronics*, 20 (1977) 7749.**
5. **Charge motion will induce signals on all electrodes, each of which will affect all the other electrodes. Handle this potential mess with:**
6. **Next: charge motion, delta rays, Ramo's theorem.**

DELTA RAYS - 1

$$\frac{d^2 n}{dTdx} = 2\pi N_A r_e^2 m_e c^2 \frac{Z}{A}\left(\frac{z}{\beta}\right)^2 \frac{F(T)}{T^2}$$

Integrating over T, the kinetic energy of the delta ray gives the number of delta rays in the 170 μm thickness of the hex sensor with T between T_1 and T_2

(T_{max} is ≈ MeV; $1/T_{max} \approx 0$)

$$T_{max} = \frac{2 m_e c^2 \beta^2 \gamma^2}{1 + 2\gamma m_e / M + (m_e / M)^2}$$ ≈ MeV; $1/T_{max} \approx 0$

$$n = 3.03(KeV)\left(\frac{1}{T_1} - \frac{1}{T_2}\right)$$

So 3 KeV δ rays are common, 30 KeV uncommon, 300 KeV rare.
Calculate production angles and then look at some of them.

DELTA RAYS - 2

- With electron velocities of about 5×10^6 cm / sec, a delta ray of length 0.5 μm
- if oriented ahead of the track
- could reach an n electrode up to 10 ps ahead of the main track.
- This will happen above 10 KeV in ≈ 5-10% of events
- These energies will be compared with the mean loss
- $dE/dx_{\mathbf{min,\ silicon}}$ = 1664 KeV / gm / cm^2 giving
- $\Delta T_{\mathbf{mean}} = 2.329 \times 0.017 \times 1664 = 65.9$ KeV.

200 3-keV delta rays

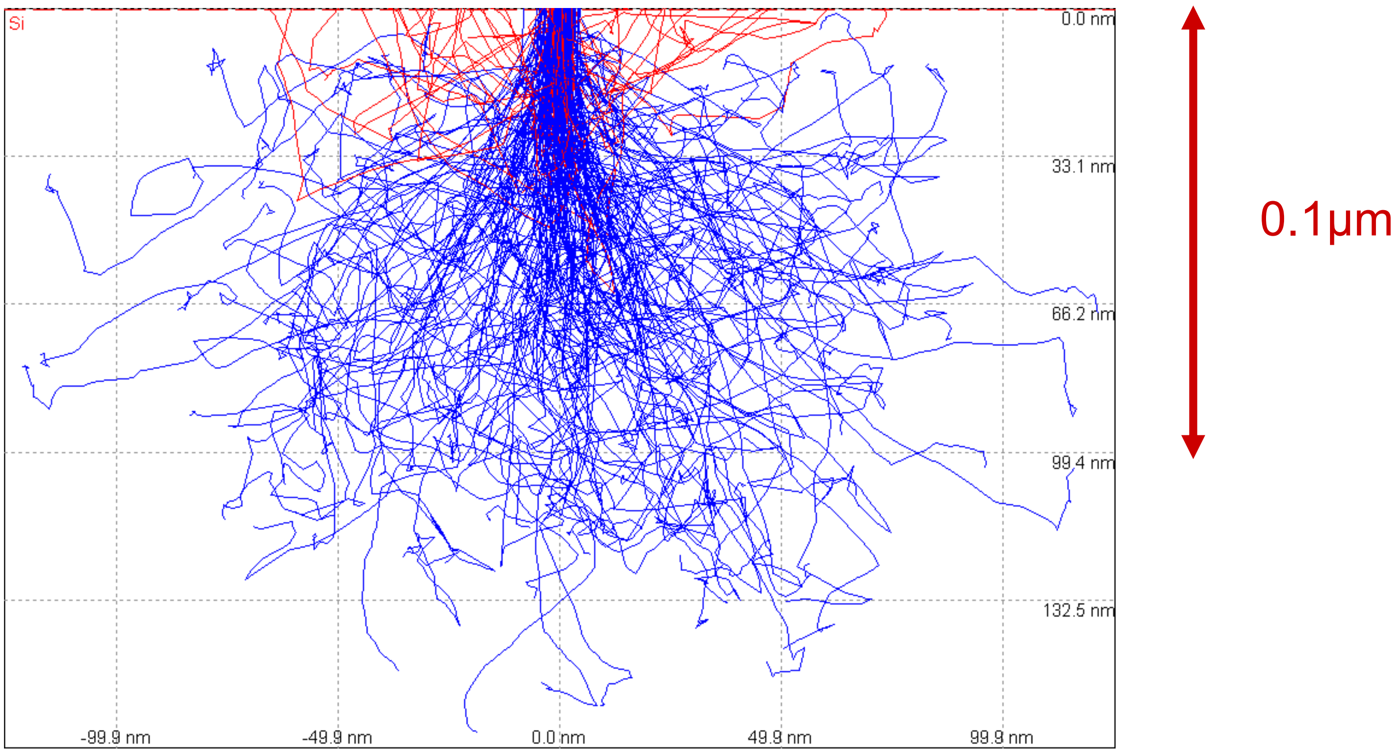

200 10-keV delta rays

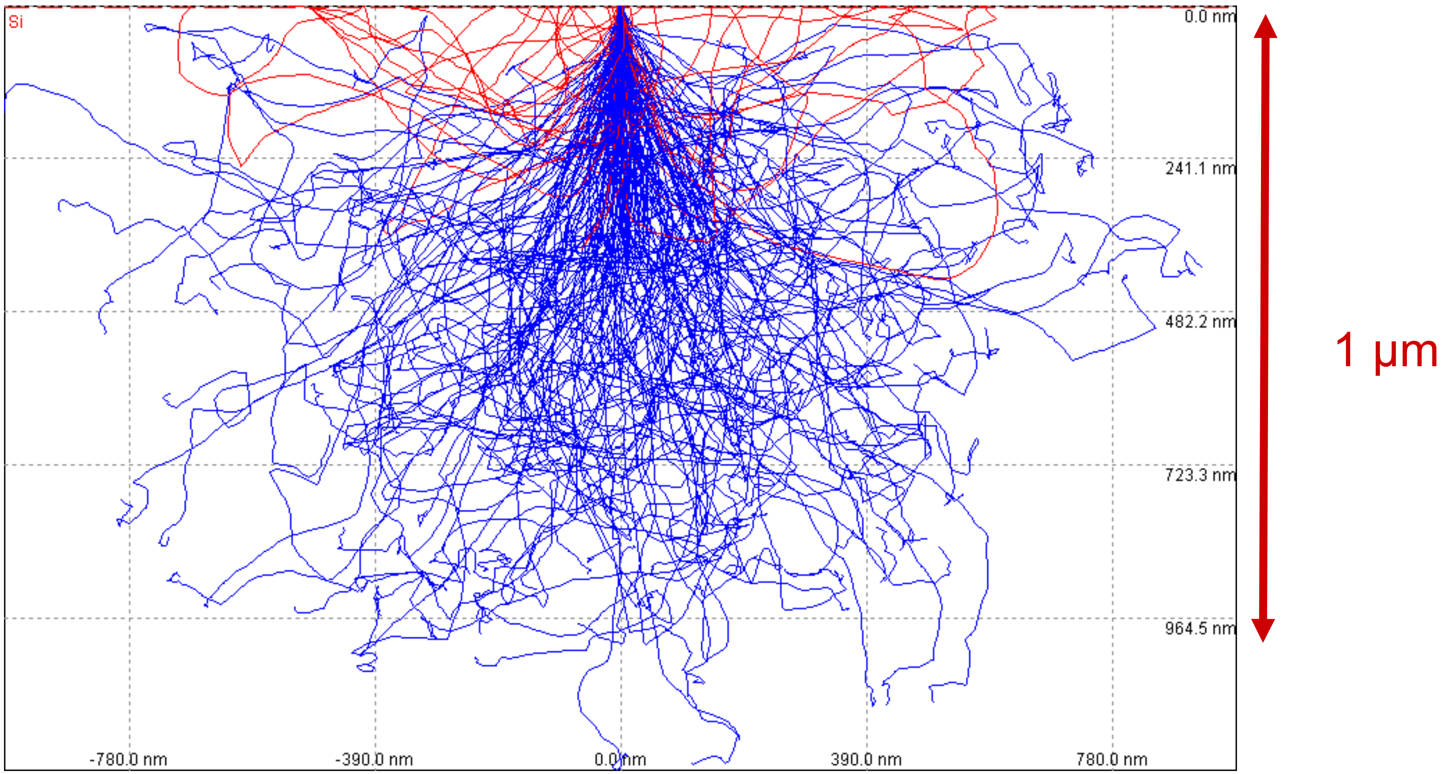

200 30-keV delta rays

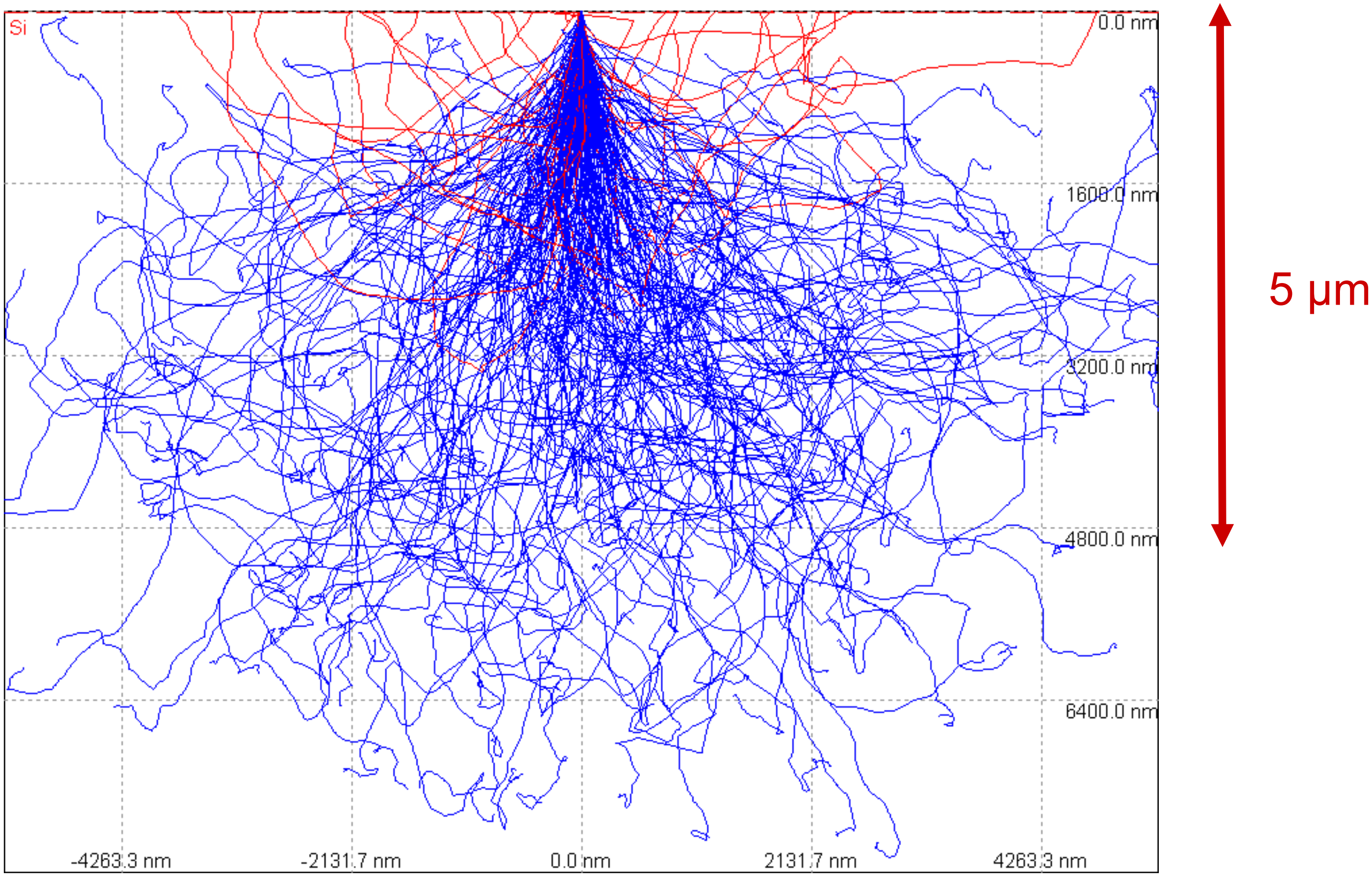

200 60-keV delta rays

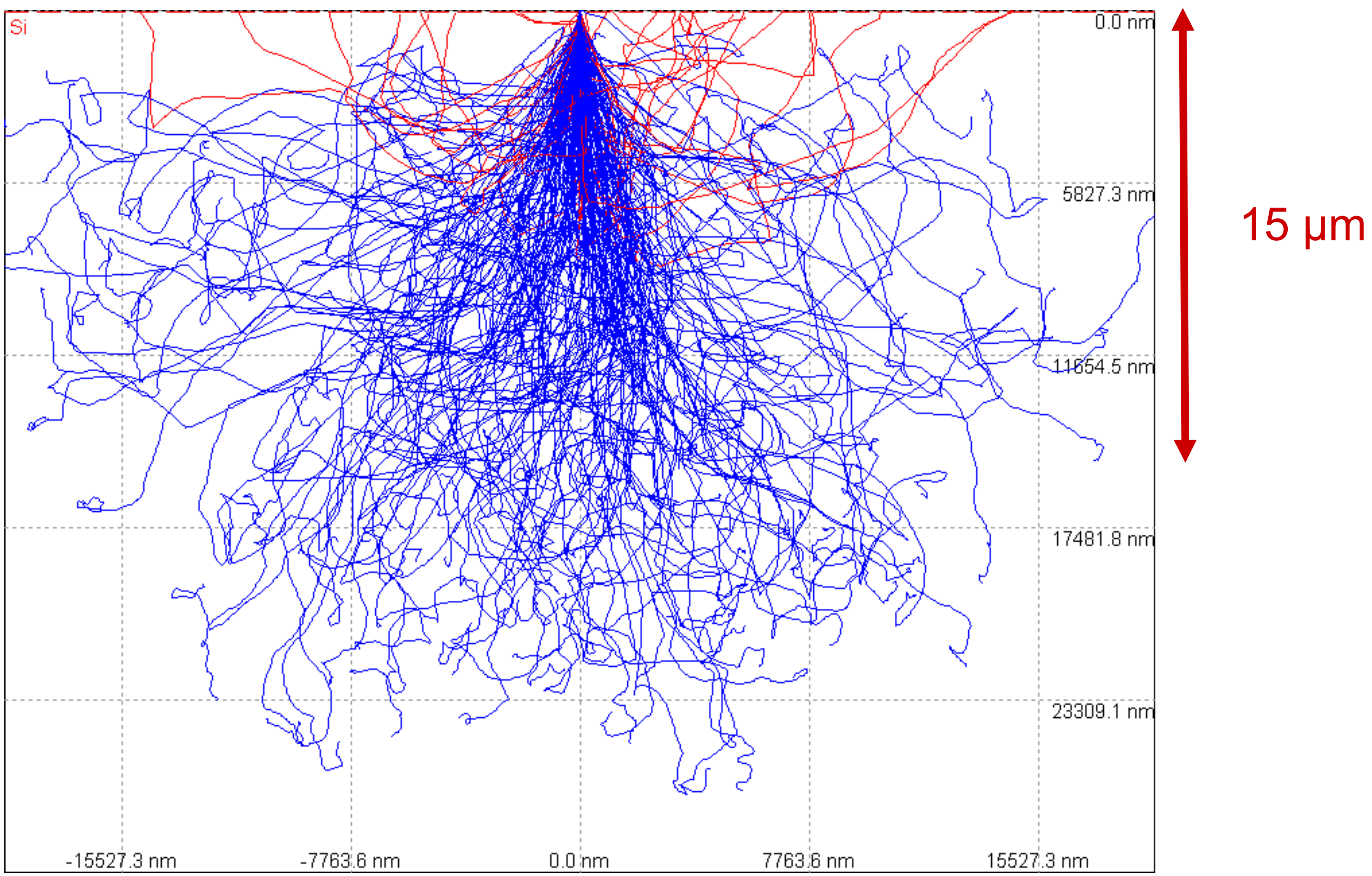

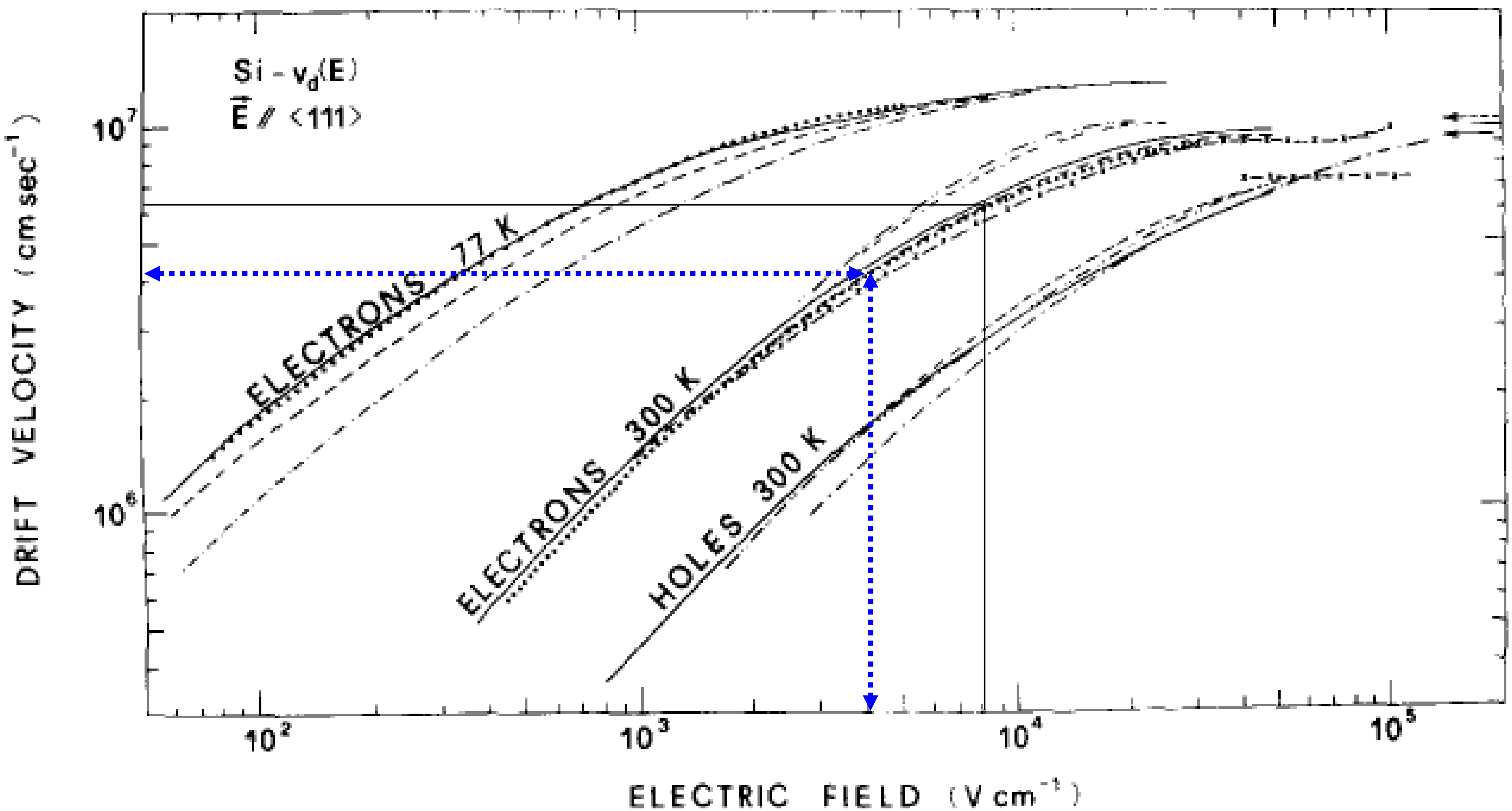

A REVIEW OF SOME CHARGE TRANSPORT PROPERTIES OF SILICON†

Solid-State Electronics, 1977, Vol. 20, pp. 77–89.

C. JACOBONI, C. CANALI, G. OTTAVIANI and A. ALBERIGI QUARANTA
Istituto di Fisica dell'Università di Modena, 41100 Modena, Italy

Velocities, diffusion, and collection times for a 100 μm parallel-plate trench electrode gap.

	electrons		holes		units
temperature	293.15	245*	293.15	245	°K
V (E = 0.5 V / μm)	4.93	7.0	2.07	2.22	cm/μs
t (E = 0.5 V / μm)	2.03	1.61	4.84	3.53	ns
σ_t, (parallel diffusion)	0.059		0.16		ns
V (E = 1.0 V / μm)	6.91	8.8	3.46	4.62	cm/μs
t (E = 1.0 V / μm)	1.45	1.21	2.89	2.22	ns
σ_t, (parallel diffusion)	0.029		0.06		ns
3 KeV δ ray (1 V / μm)	1.9	1.5	3.8	2.8	ps
10 KeV δ ray (1 V / μm)	14	11	29	22	ps
30 KeV δ ray (1 V / μm)	101	80	202	152	ps
60 KeV δ ray (1 V / μm)	362	284	723	541	ps

Calculations based on material in:

A REVIEW OF SOME CHARGE TRANSPORT PROPERTIES OF SILICON

***Solid-State Electronics* 20 (1977) 77 – 89**

C. Jacoboni, C. Canali, G. Ottaviani and A. Alberigi Quaranta

1. introduction
2. history
3. factors affecting speed
4. generating the signal – Ramo’s theorem
5. amplifying the signal – charge and current amplifiers
6. trench electrode sensors
7. hex-cell sensors
8. experimental results
9. analysis – constant fraction discrimination
10. analysis – fitting with almost-noise-free pulses
11. next

0.13 μm chips now fabricated and used here
rise, fall times ≈ 1.5 ns

A high-speed low-noise transimpedance amplifier in a 0.25 μm CMOS technology

Giovanni Anelli[a,*], Kurt Borer[b], Luca Casagrande[a], Matthieu Despeisse[a], Pierre Jarron[a], Nicolas Pelloux[a], Shahyar Saramad[a,c]

rise times ≈ 3.5 ns **fall times ≈ 3.5 ns**

[a] *CERN, EP Division, CH-1211 Geneva 23, Switzerland*

[b] *University of Bern, Laboratory for High Energy Physics, Sidlerstr. 5, CH-3012 Bern, Switzerland*

[c] *Institute for Studies in Theoretical Physics and Mathematics (IPM), Tehran, Iran, P.O. Box 19395-5531*

Elsevier use only: Received date here; revised date here; accepted date here

Abstract

We present the simulated and measured performance of a transimpedance amplifier designed in a quarter micron CMOS process. Containing only NMOS and PMOS devices, this amplifier can be integrated in any submicron CMOS process. The main feature of this design is that a transistor in the feedback path substitutes the transresistance. The circuit has been optimized for reading signals coming from silicon strip detectors with few pF input capacitance. For an input charge of 4 fC, an input capacitance of 4 pF and a transresistance of 135 kΩ, we have measured an output pulse fall time of 3 ns and an Equivalent Noise Charge (ENC) of around 350 electrons rms. In view of a utilization of the chip at cryogenic temperatures, measurements at 130 K have also been carried out, showing an overall improvement in the performance of the chip. Fall times down to 1.5 ns have been measured. An integrated circuit containing 32 channels has been designed and wire-bonded to a silicon strip detector and successfully used for the construction of a high-intensity proton beam hodoscope for the NA60 experiment. The chip has been laid out using special techniques to improve its radiation tolerance, and it has been irradiated up to 10 Mrd (SiO_2) without showing any degradation in the performance.

Keywords: Deep submicron; CMOS; Transimpedance amplifier; Radiation tolerance; Low temperature CMOS

1. **introduction**
2. **history**
3. **factors affecting speed**
4. **generating the signal – Ramo's theorem**
5. **amplifying the signal – charge and current amplifiers**
6. **trench electrode sensors**
7. **hex-cell sensors**
8. **experimental results**
9. **analysis – constant fraction discrimination**
10. **analysis – fitting with almost-noise-free pulses**
11. **next**

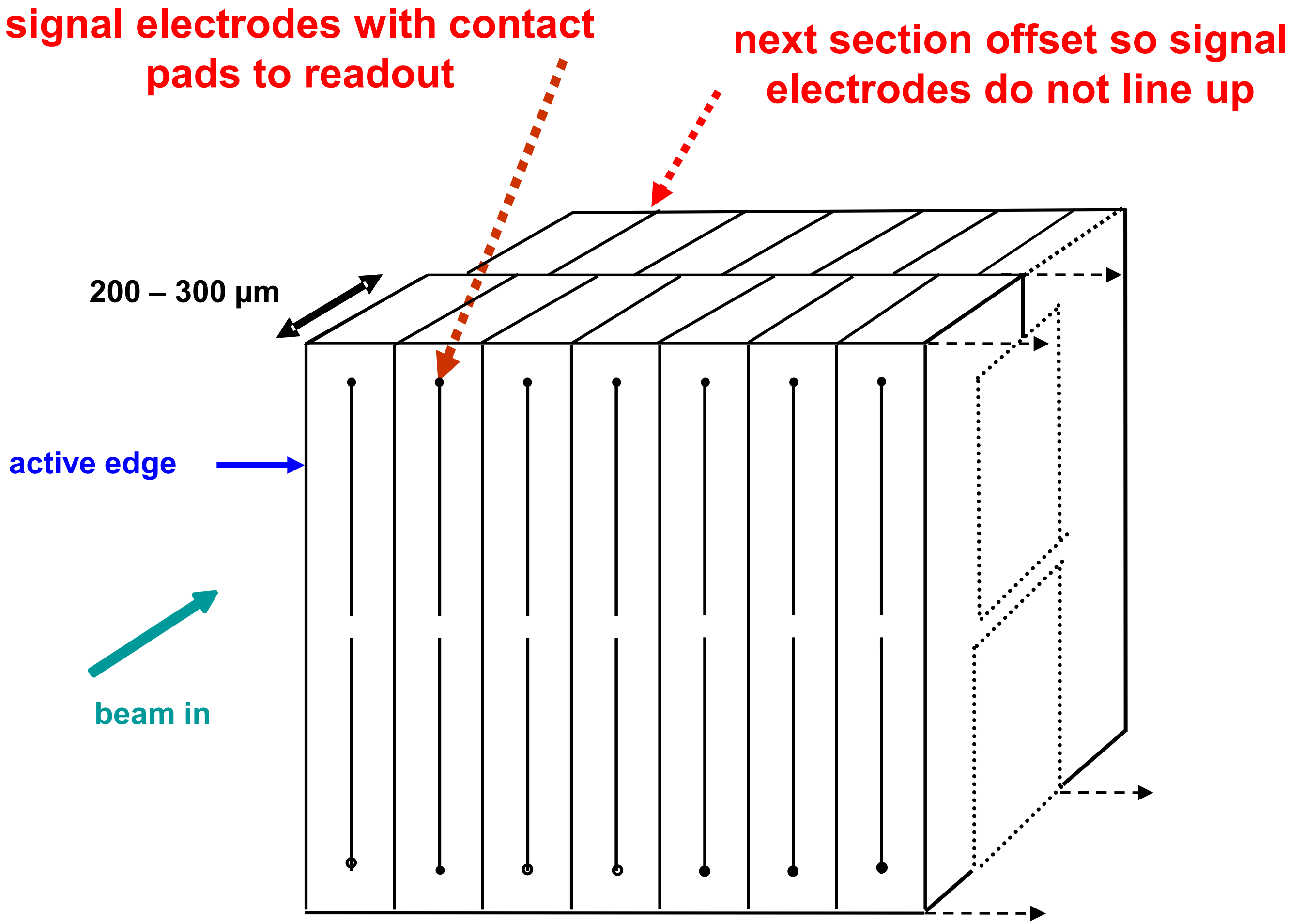

Schematic diagram of part of one section of two of the planes in an active-edge 3D trench-electrode detector. Other offsets (⅓, ⅔, 0, ⅓, ⅔ ..etc.) may also be used.

A trench-electrode sensor will have:

- high average field / peak field,
- a uniform Ramo weighting field,
- an initial pulse time that is independent of the track position and,
- for two facing 100 μm gaps with a common electrode and a 250 μm thickness (in the track direction) a capacitance of 0.527 pF per mm of height.
- For moderate to high bias voltage levels (~ 50 V) and low dopant levels (~ 5 $\times 10^{11}$ / cm^3) we can neglect $V_{depletion} \approx 2$ V, and assume a constant charge-carrier drift velocity. After irradiation, drift velocities will not be uniform, but will be faster as we raise the bias voltage.

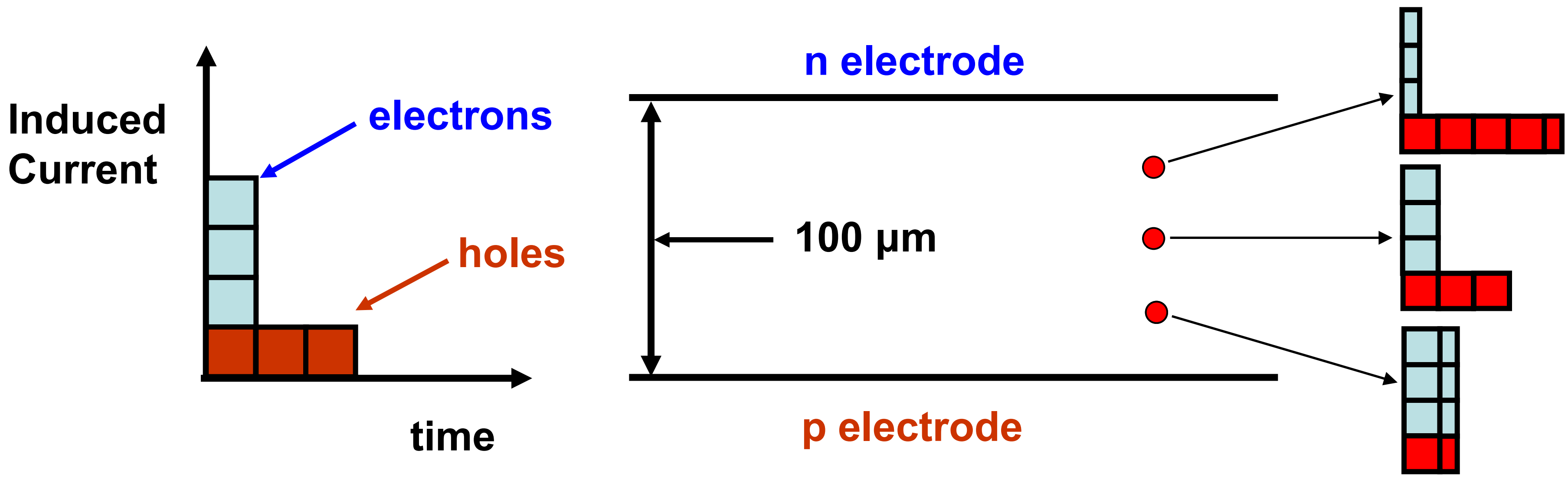

Schematic, idealized diagram of induced currents from tracks in a parallel-plate trench-electrode sensor.

Tracks (●) are perpendicular, at the mid and quarter points.

Velocity (electrons) ≡ 3.0 × Velocity (holes).

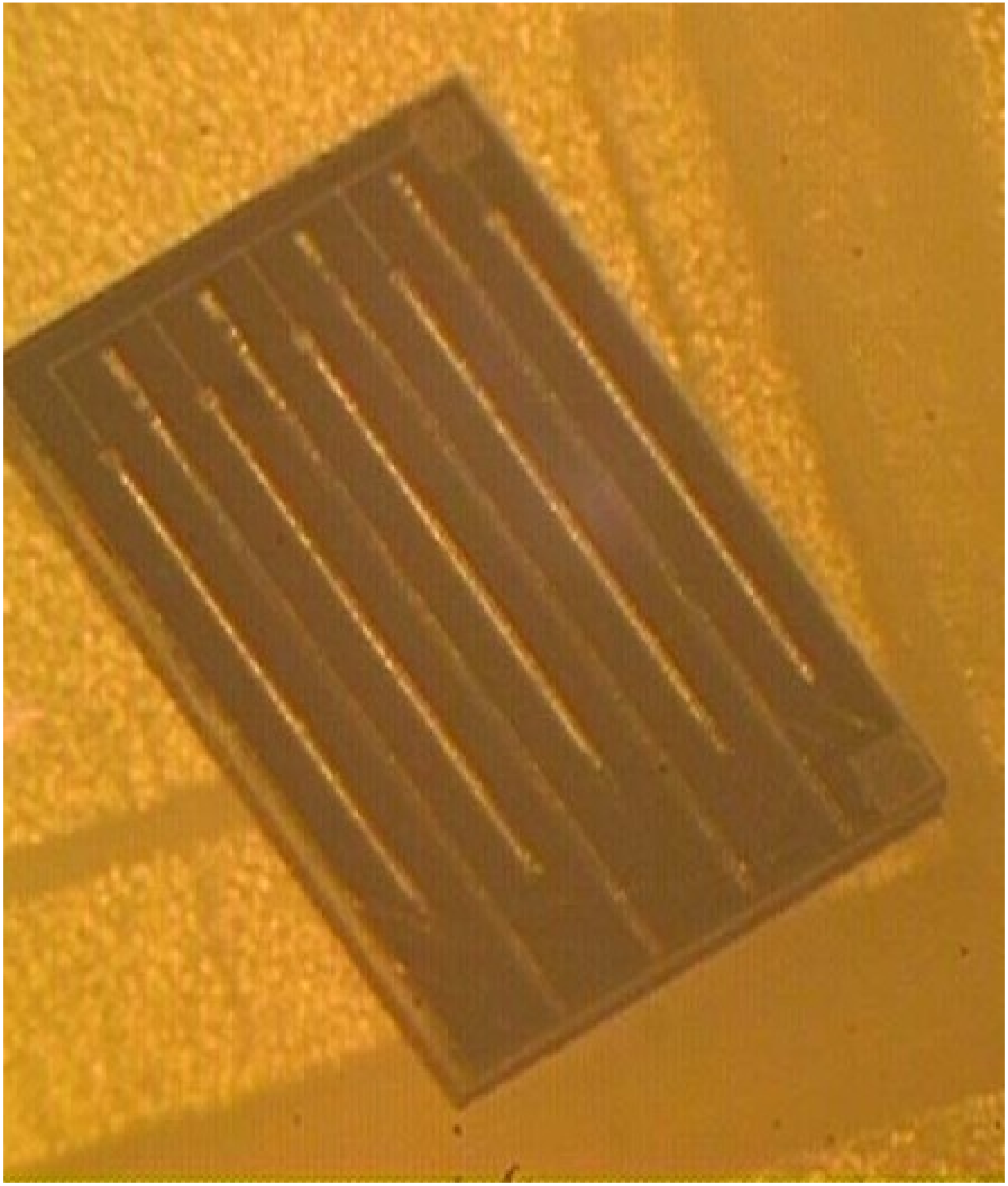

SLAC Mask

FE-I4 Sensor: 8

FE-I3 Sensors: 9

FE-I4 geometry test sensors: 55

Trench Sensors:
12: 50 um n-2-p pitch, 1 mm long, 64 channels

5: 50 um n-2-p pitch, 5 mm long, 64 channels

23: 100 n-2-p pitch, 3 mm long, 16 channels

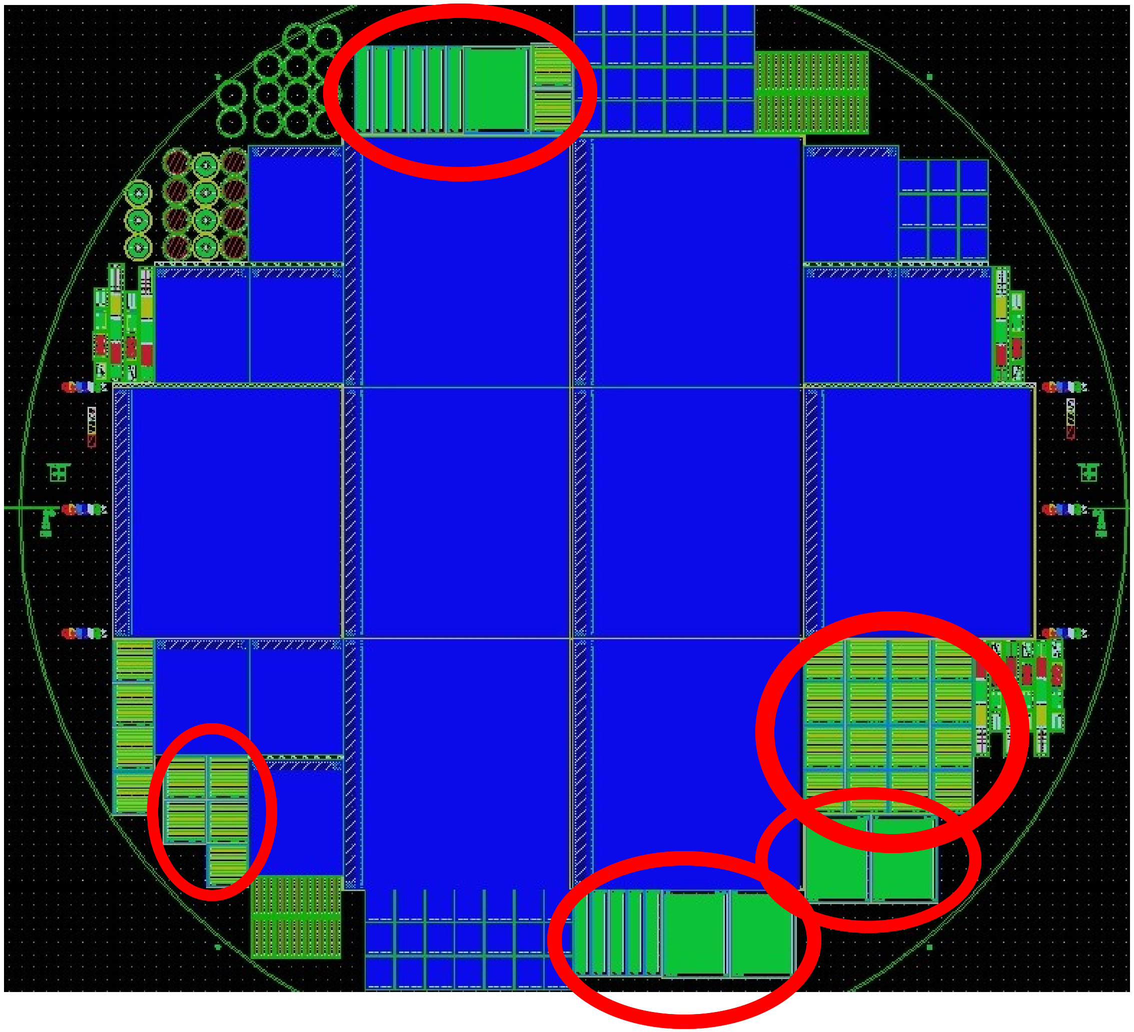

Fast Timing Example

Effort was made to pinch-off and isolate both types of trenches by deleting the surfaces of p-spray. So both electron and hole signals can be readout separately.

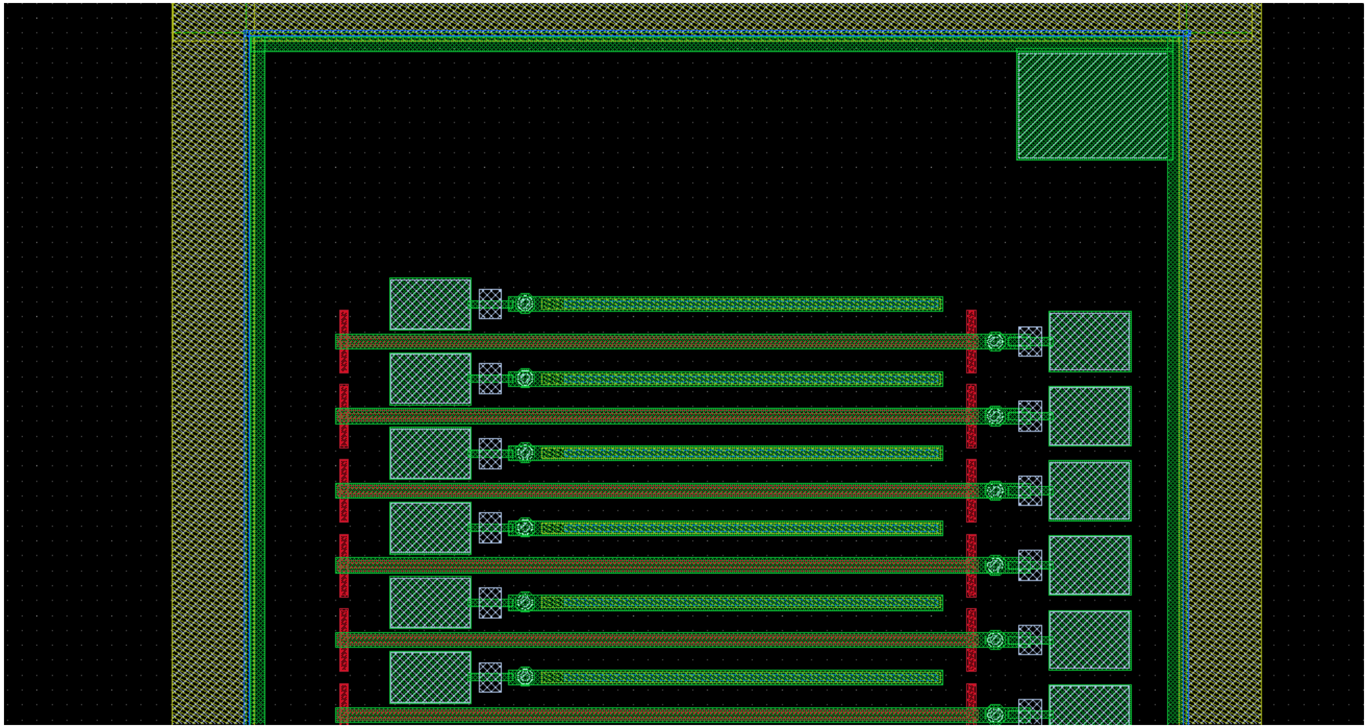

Fast Timing Example

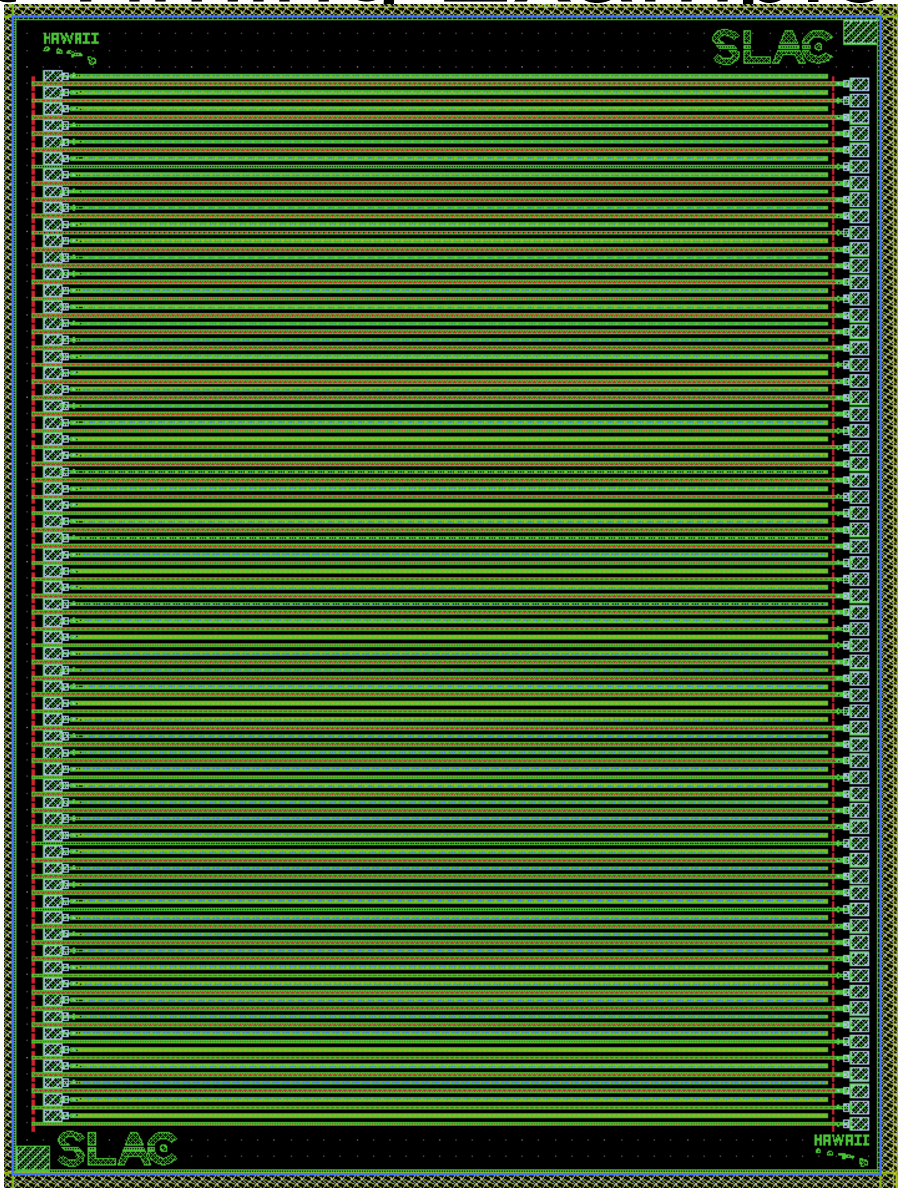

1. **introduction**
2. **history**
3. **factors affecting speed**
4. **generating the signal – Ramo's theorem**
5. **amplifying the signal – charge and current amplifiers**
6. **trench electrode sensors**
7. **hex-cell sensors**
8. **experimental results**
9. **analysis – constant fraction discrimination**
10. **analysis – fitting with almost-noise-free pulses**
11. **next**

But for now we used a 50 μm-side hex sensor (following slides)

1. with 20 V bias, at room temperature - 40V should be ok,
2. with each column of hexagons tied to a 0.13 μm current-amplifier channel (so large capacitance),
3. exposed to an uncollimated ^{90}Sr beta source,
4. output to an oscilloscope triggered by the signal itself.

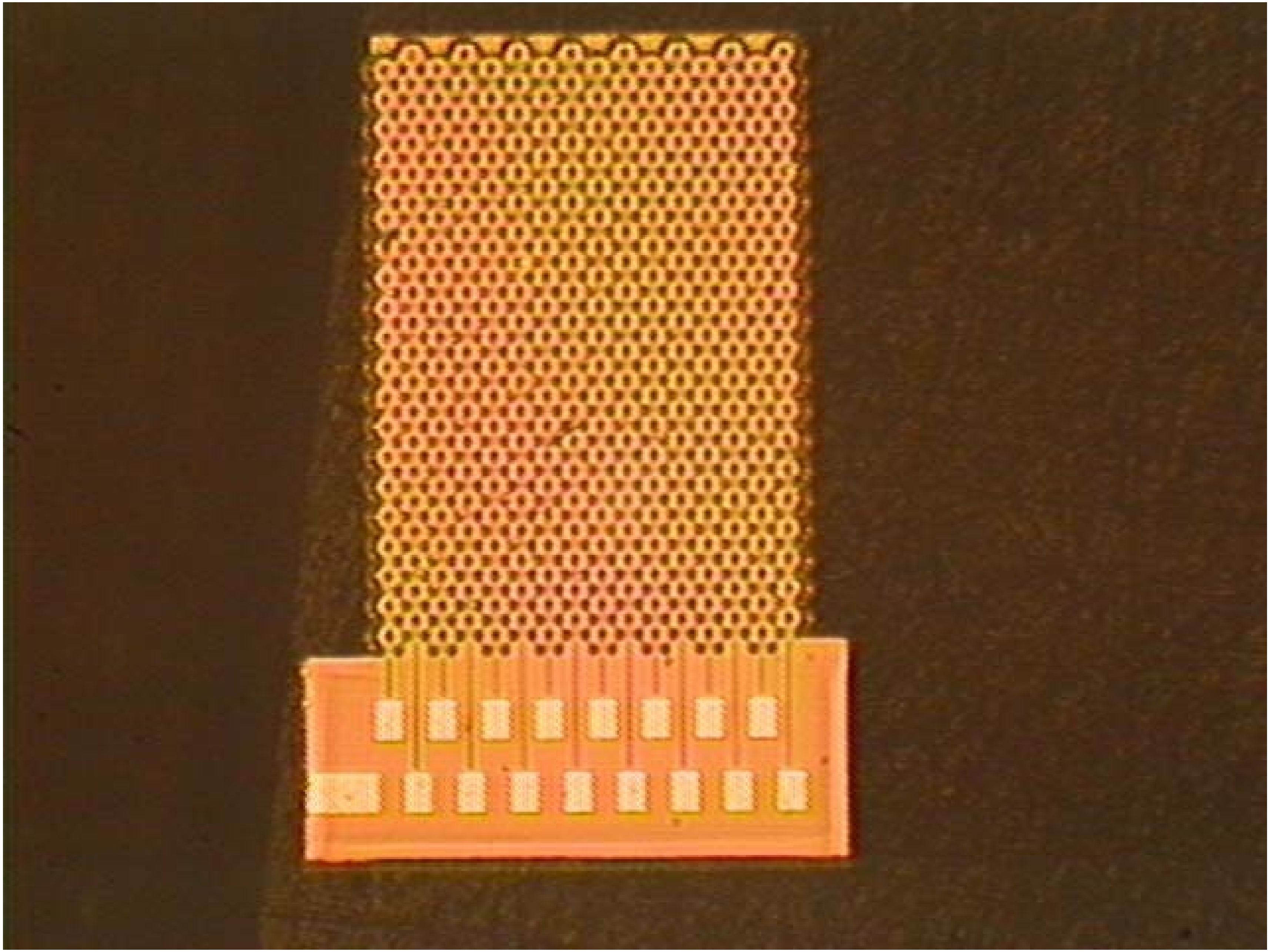

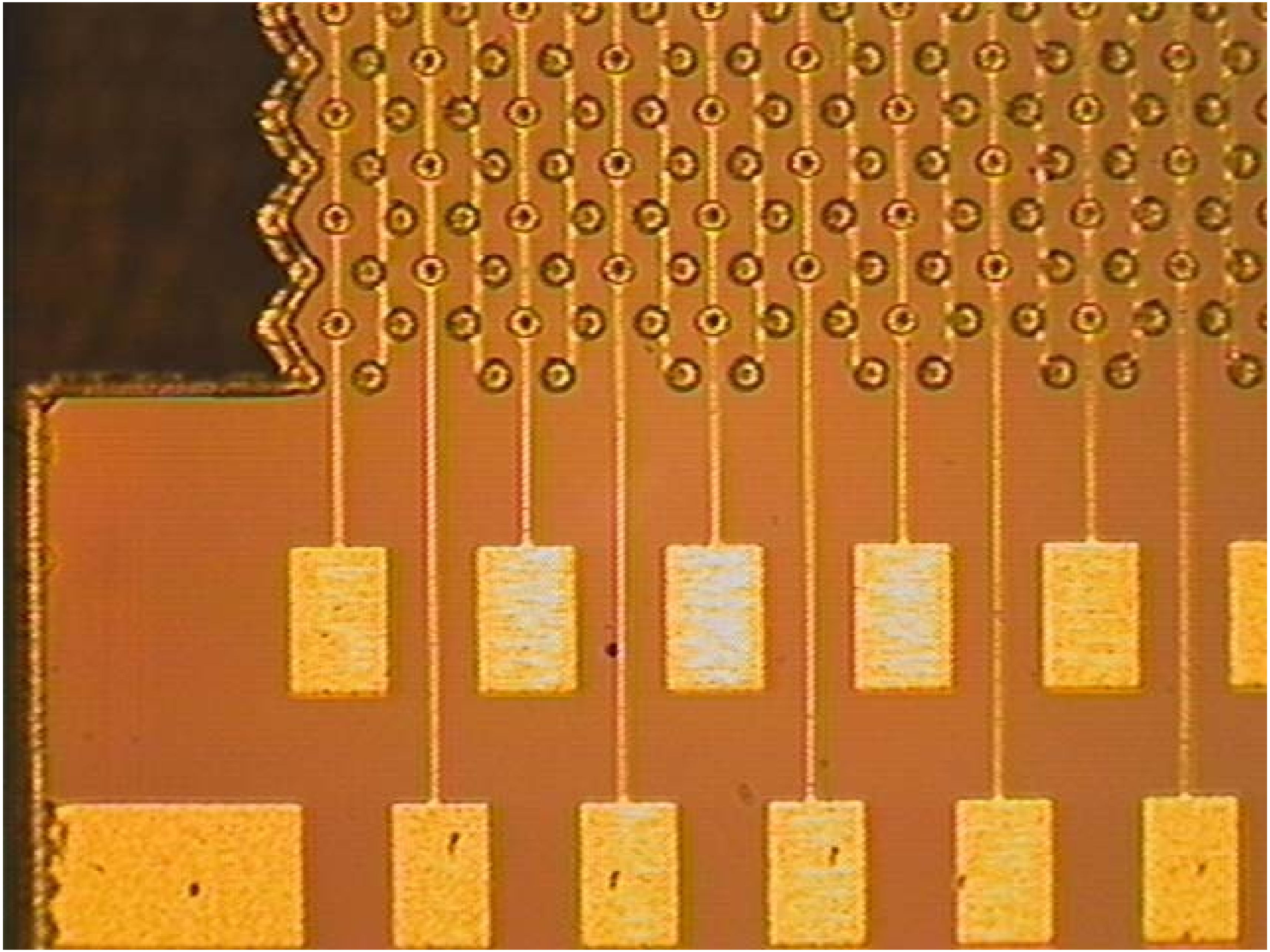

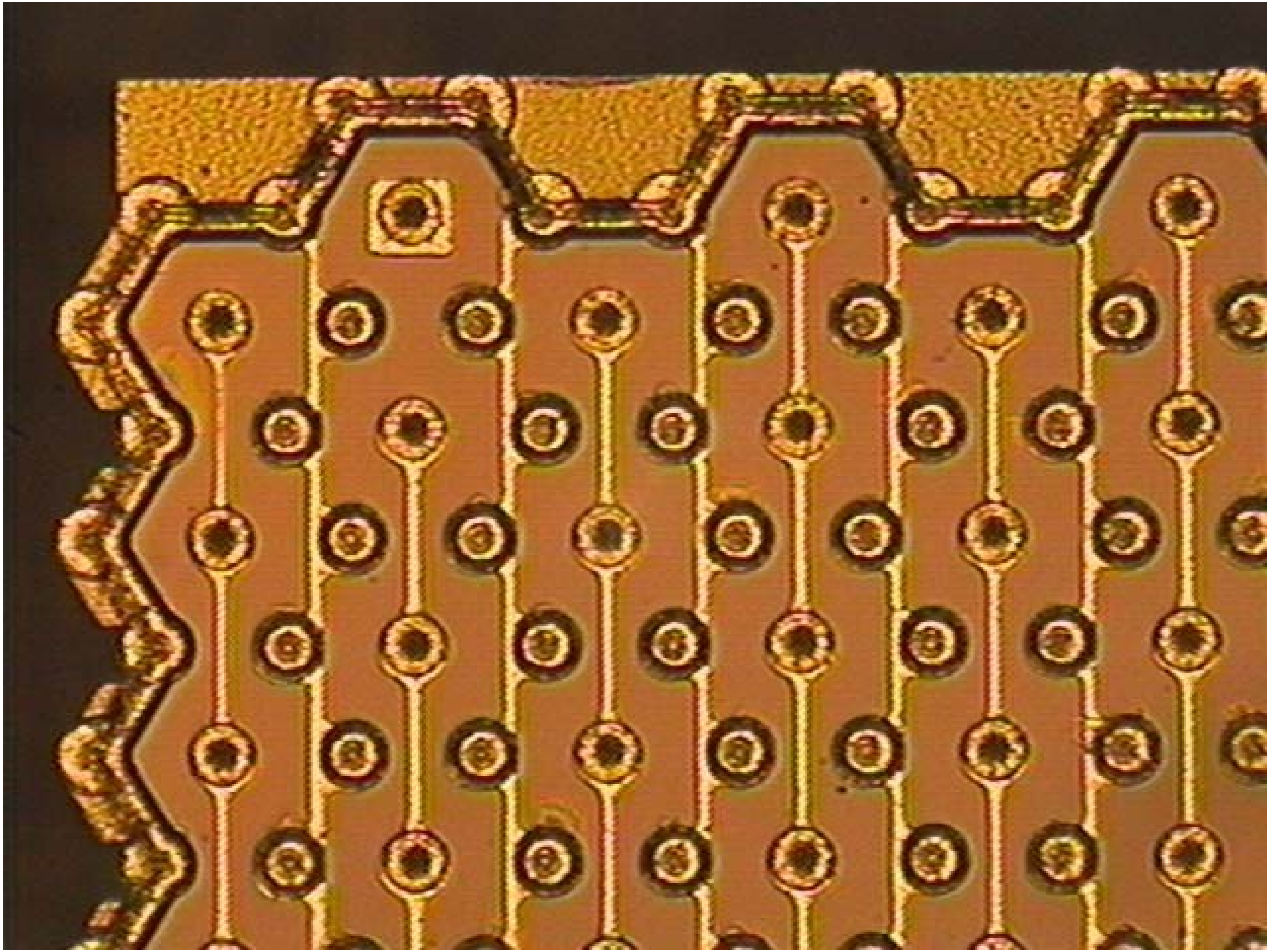

1. **introduction**
2. **history**
3. **factors affecting speed**
4. **generating the signal – Ramo's theorem**
5. **amplifying the signal – charge and current amplifiers**
6. **trench electrode sensors**
7. **hex-cell sensors**
8. **experimental results**
9. **analysis – constant fraction discrimination**
10. **analysis – fitting with almost-noise-free pulses**
11. **next**

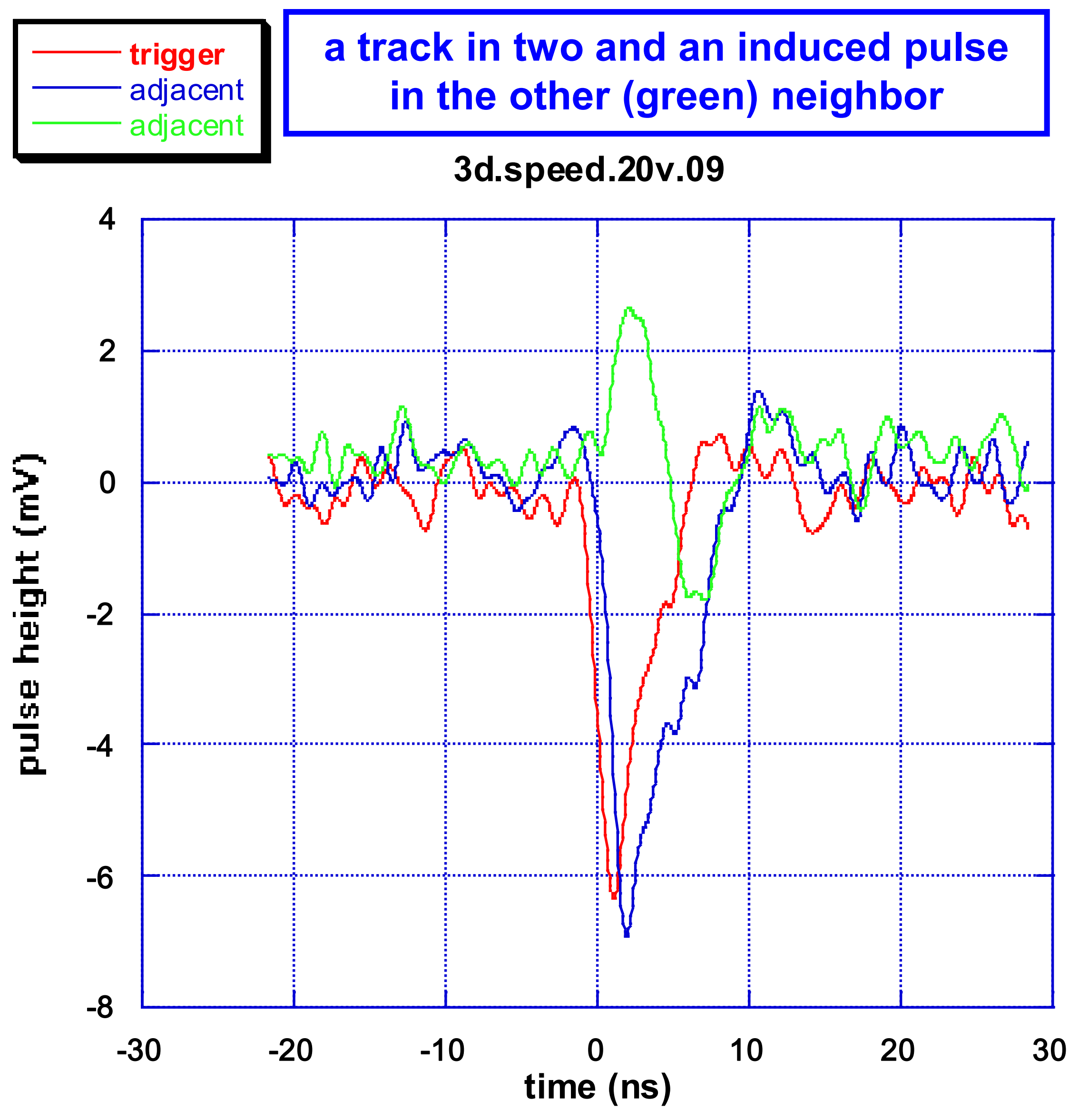
trigger
adjacent
adjacent
a track in two and an induced pulse
in the other (green) neighbor
3d.speed.20v.09
4
2
0
-2
-4
-6
-8
pulse height (mV)
-30
-20
-10
0
10
20
30
time (ns)

First, one problem with betas: an example of a possible angled track distorting the pulse shape. (We will need real test beam data)

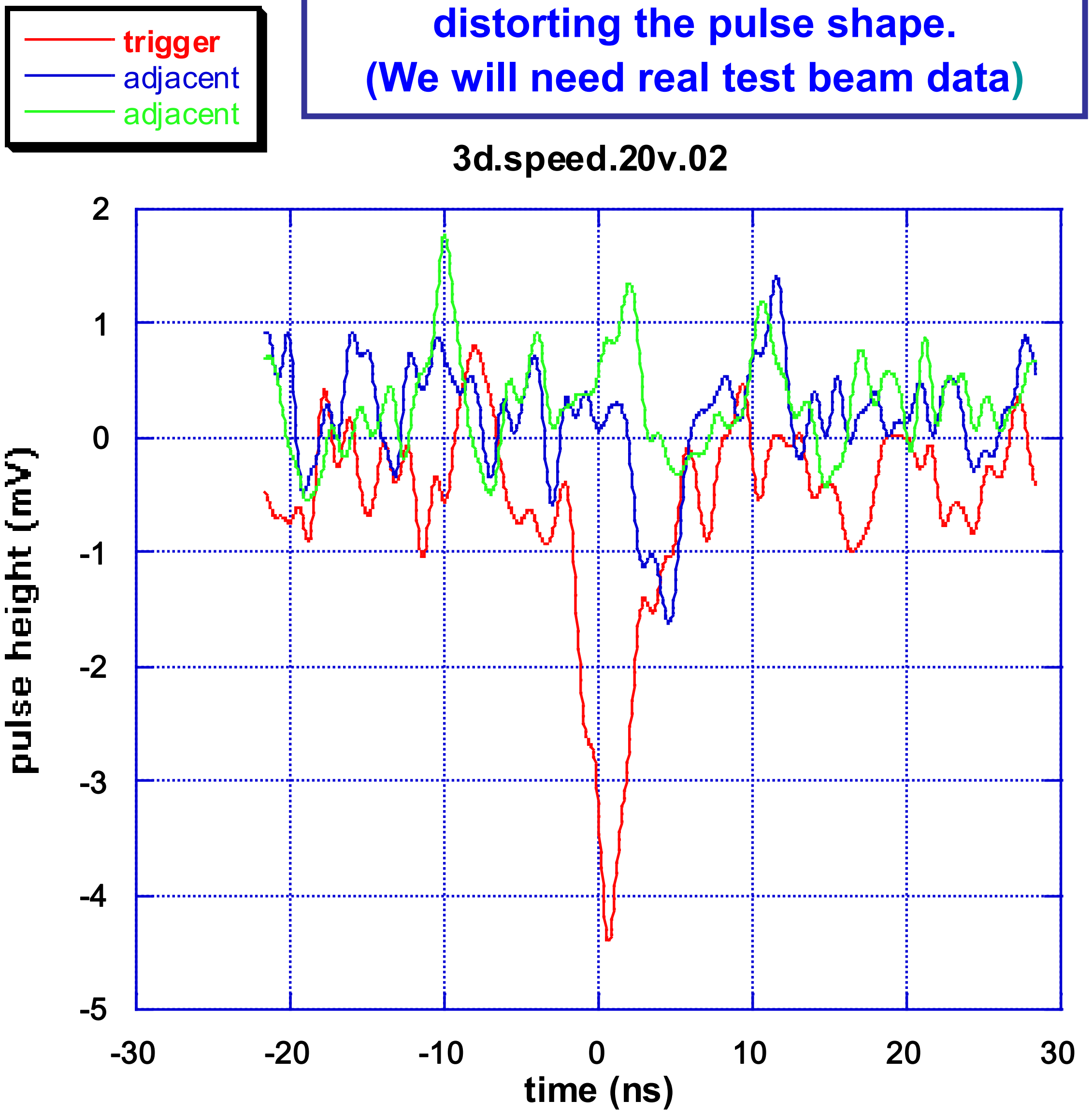

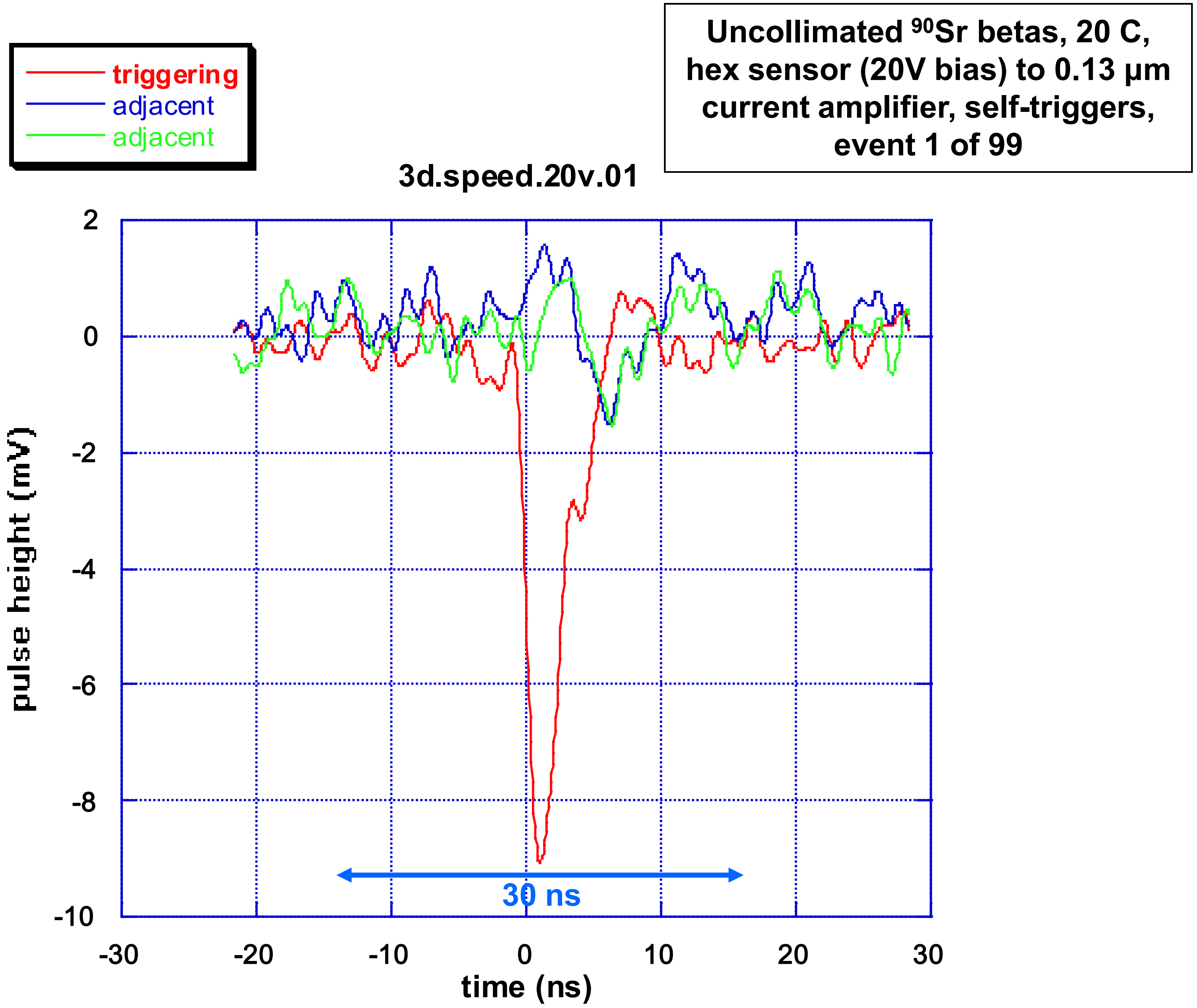

triggering
adjacent
adjacent
Uncollimated 90Sr betas, 20 C, hex sensor (20V bias) to 0.13 µm current amplifier, self-triggers, event 1 of 99
3d.speed.20v.01
2
0
-2
-4
-6
-8
-10
pulse height (mV)
30 ns
-30
-20
-10
0
10
20
30
time (ns)

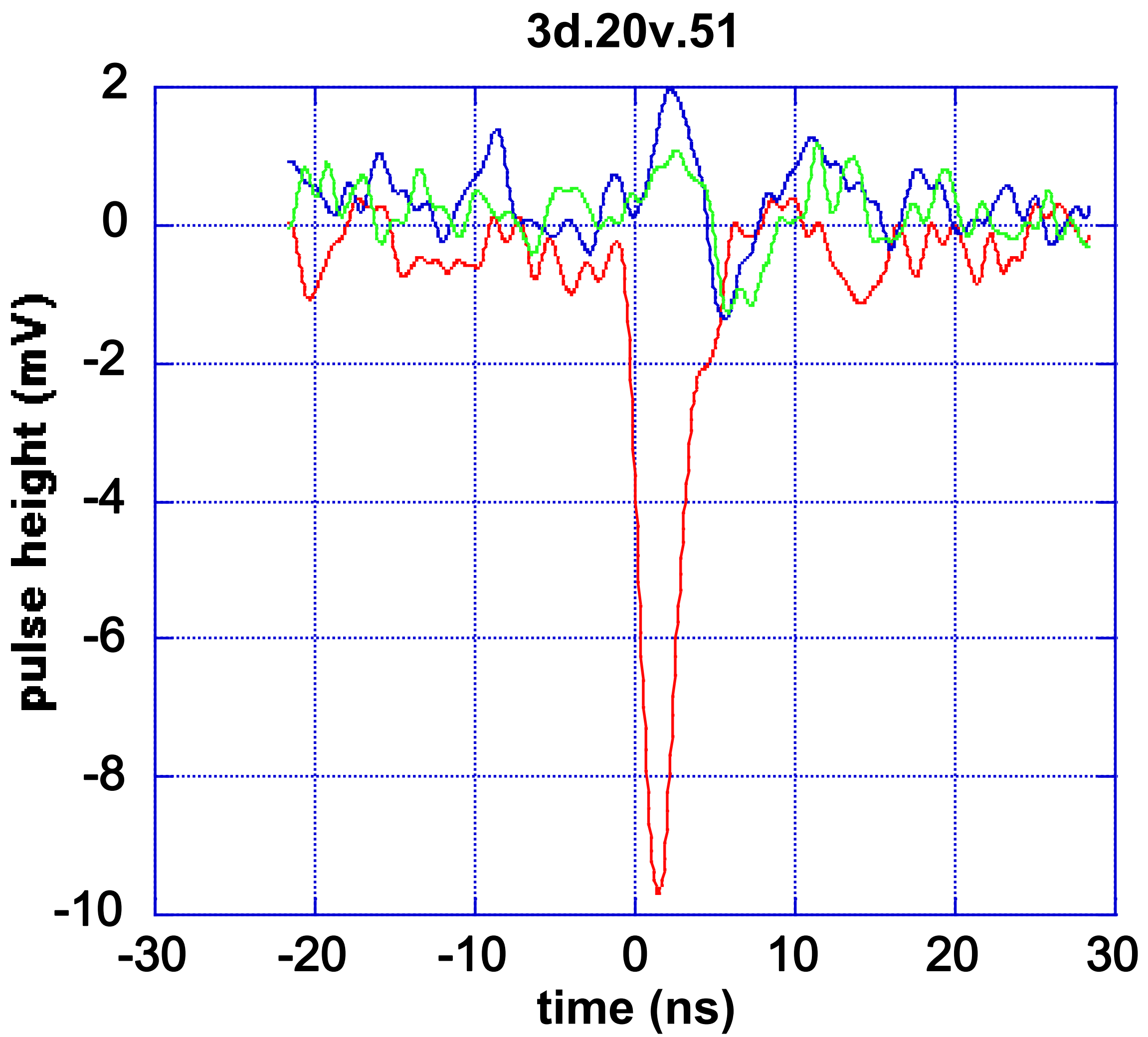

The middle event

Uncollimated ^{90}Sr betas, 20 C, hex sensor (20V bias) to 0.13 μm current amplifier, self-triggers, event 99 of 99

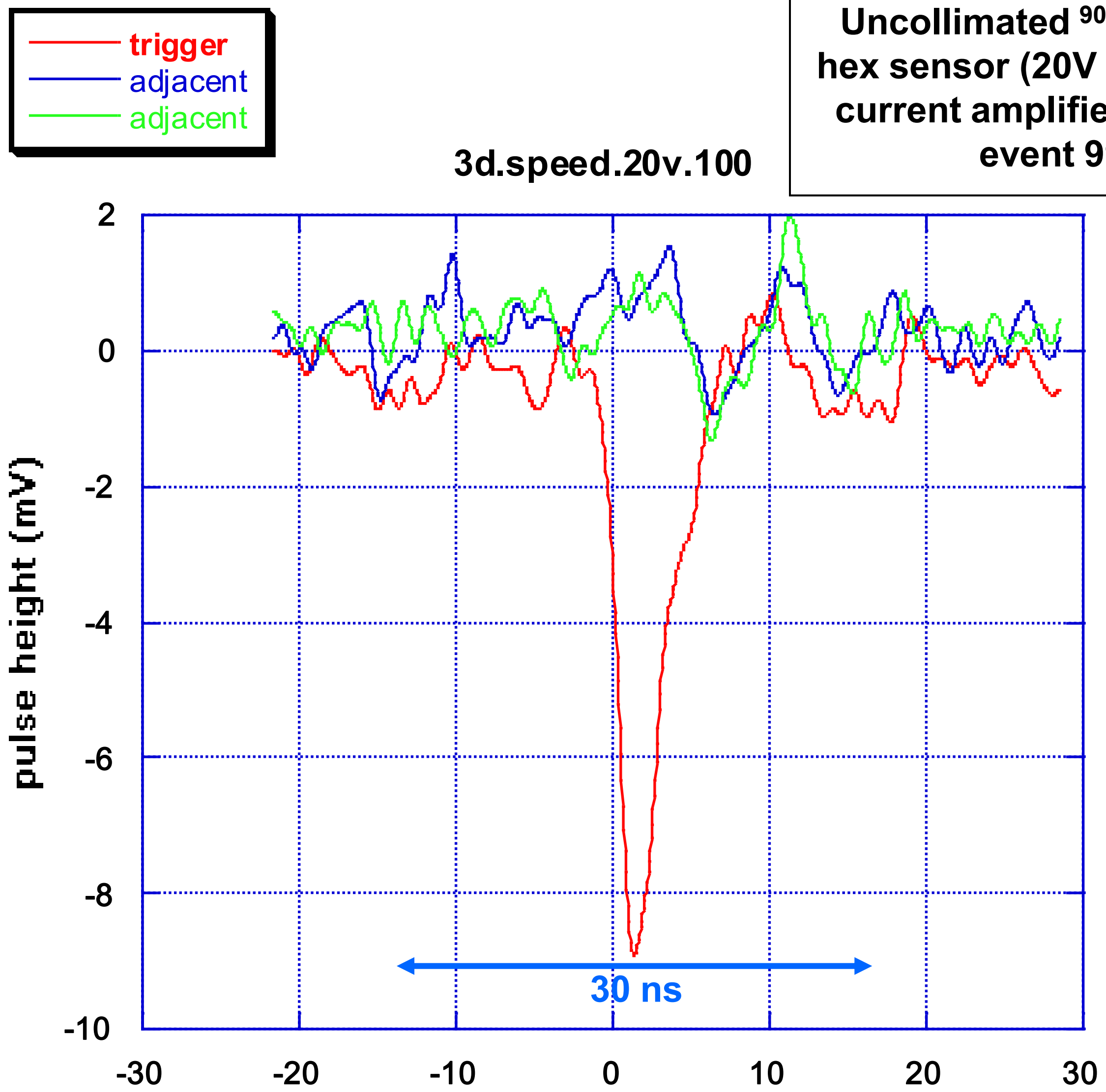

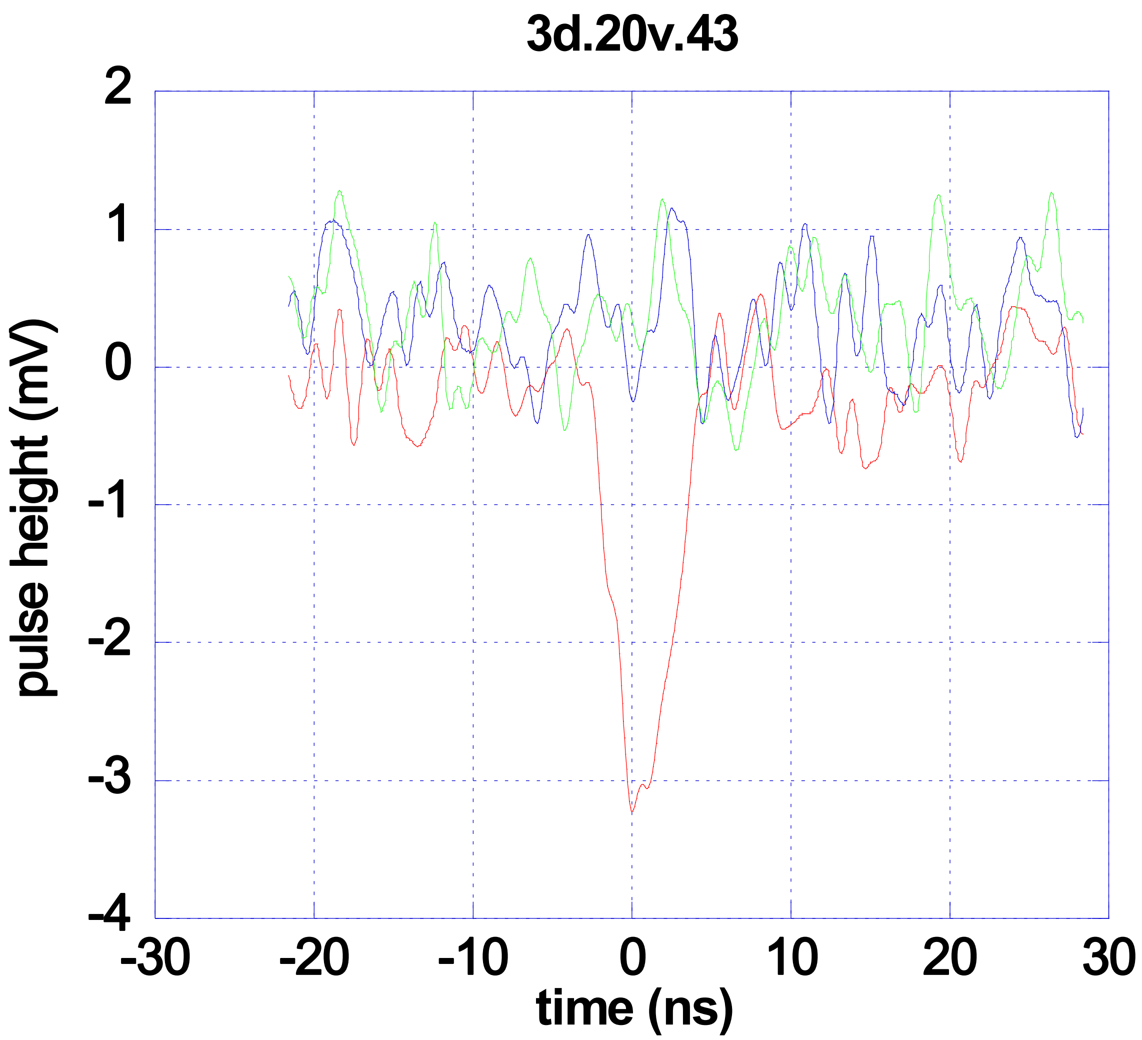

The single-column event with the largest expected timing error in the central scatter plot.

Pulse shape from the sum of the 6 largest pulses. τ-rise = 1.6 ns, fwhm = 2.90 ns. Note the trailing edge hole current, and amplifier ringing.

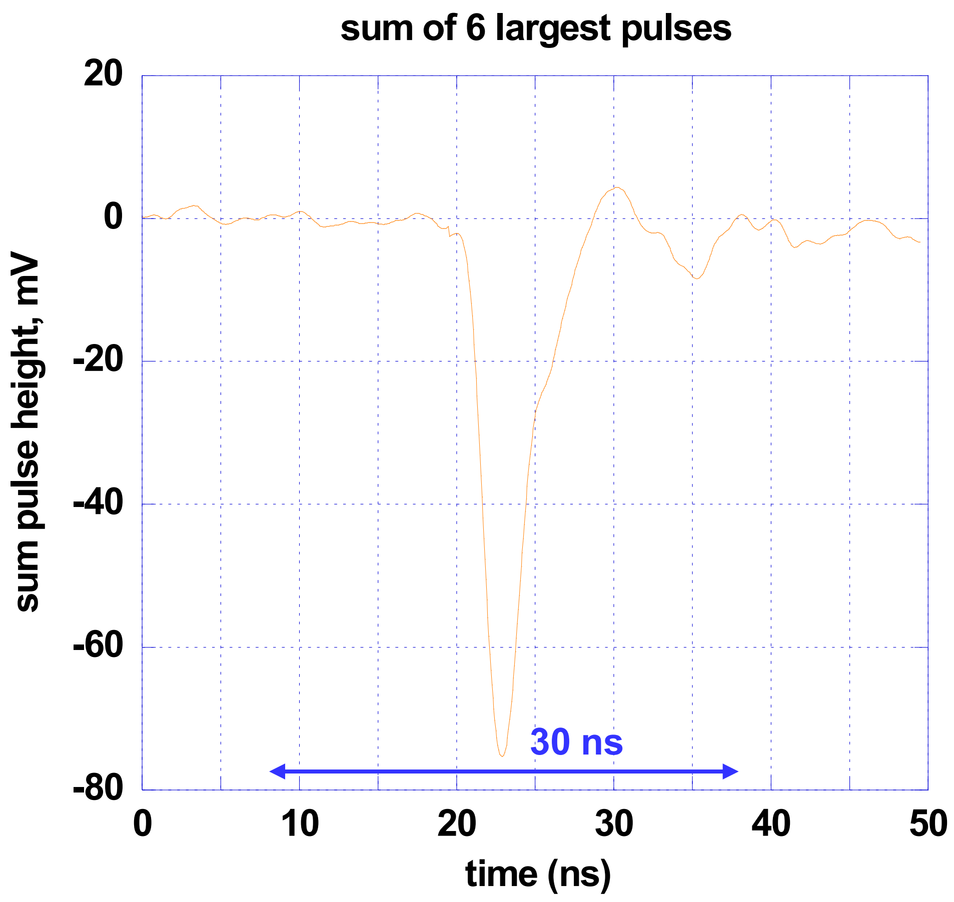

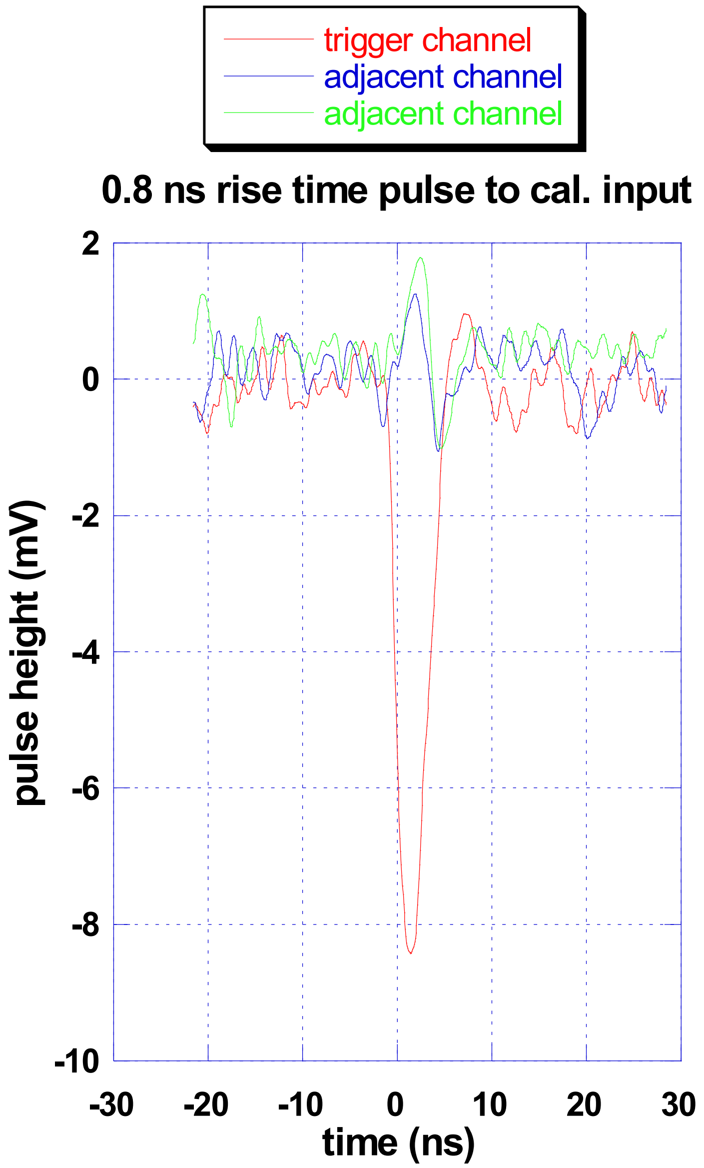

With a pulse from a pulse generator, with the 10% and 90% time points only 0.8 ns apart, we see an amplifier rise time of 1.5 ns. Sensor signals have rise times of 1.6 ns. So the amplifier is currently the limiting element.

1. introduction
2. history
3. factors affecting speed
4. generating the signal – Ramo’s theorem
5. amplifying the signal – charge and current amplifiers
6. trench electrode sensors
7. hex-cell sensors
8. experimental results
9. analysis – constant fraction discrimination
10. analysis – fitting with almost-noise-free pulses
11. next

Estimate the time resolution at room temperature with

- **the hex sensor, and**
- **a preliminary version of a 0.13 μm integrated circuit readout**
- **using data from un-collimated 90-Sr βs (but only with tracks in the central channel).**
- **(A wall-electrode with parallel plates would give shorter times, but the hex sensor already has almost the same output rise time as a 0.8 ns input rise time pulse generator, so the output shape is primarily determined by the amplifier, not the sensor).**
- **To simulate a constant fraction discriminator set at 50% (where slope is steepest):**
- **Fit leading baseline, and measure noise,**
- **Fit top and find halfway point,**
- **ΔT = σ-noise / slope**
- **With wall-electrode sensor and a parallel beam,**
- **can do better fitting entire pulse.**

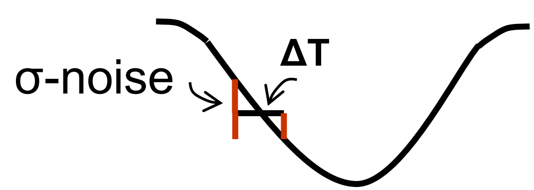

Noise distribution from pre-pulse region with a Gaussian fit.

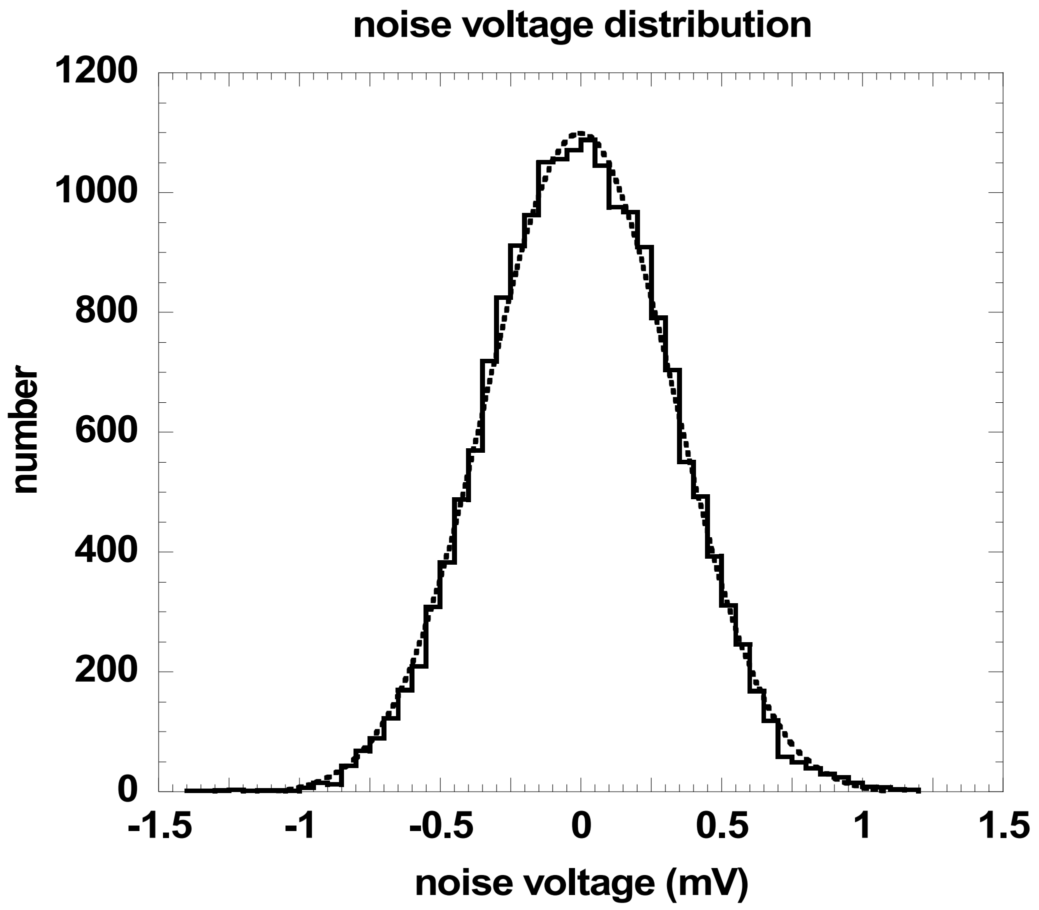

Noise distribution from pre-pulse with a Gaussian fit – log scale to show tails

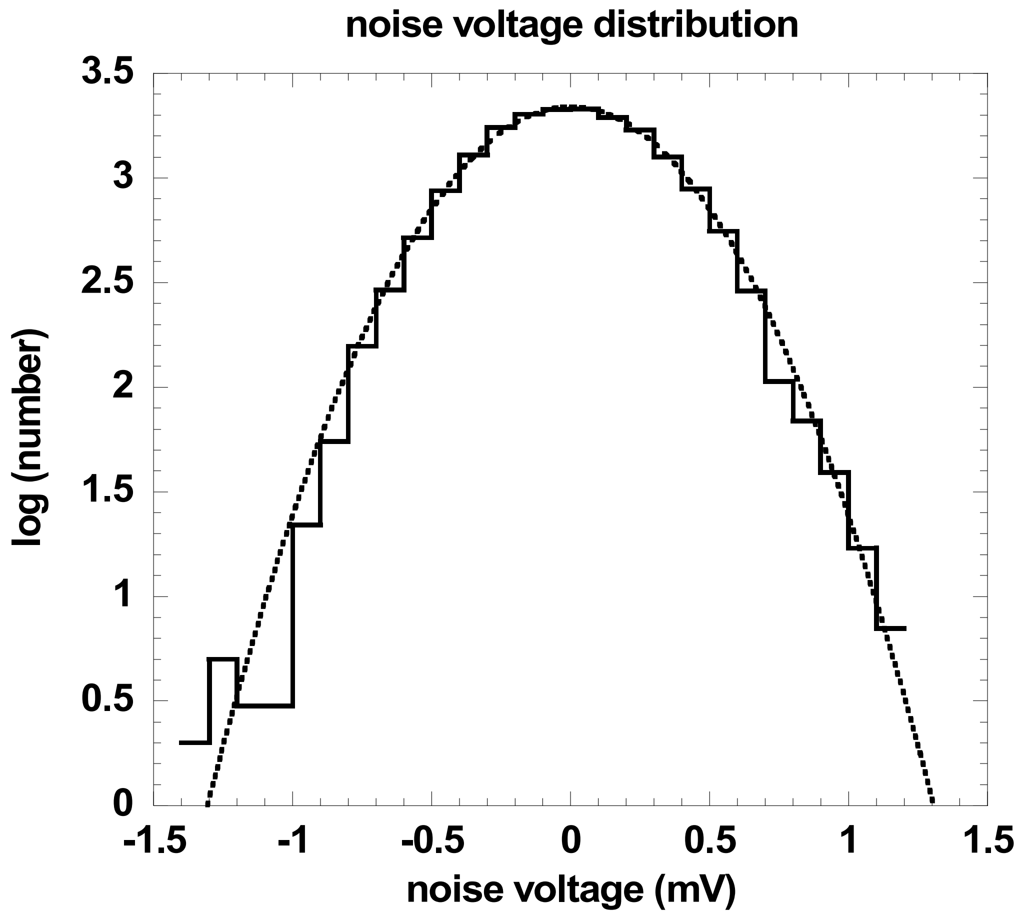

sigma = 0.33166 +/- 0.0033 mV

direct standard deviation from the18,090 voltage values = 0.3218 mV

Fourier transform of noise: Gaussian, but not white

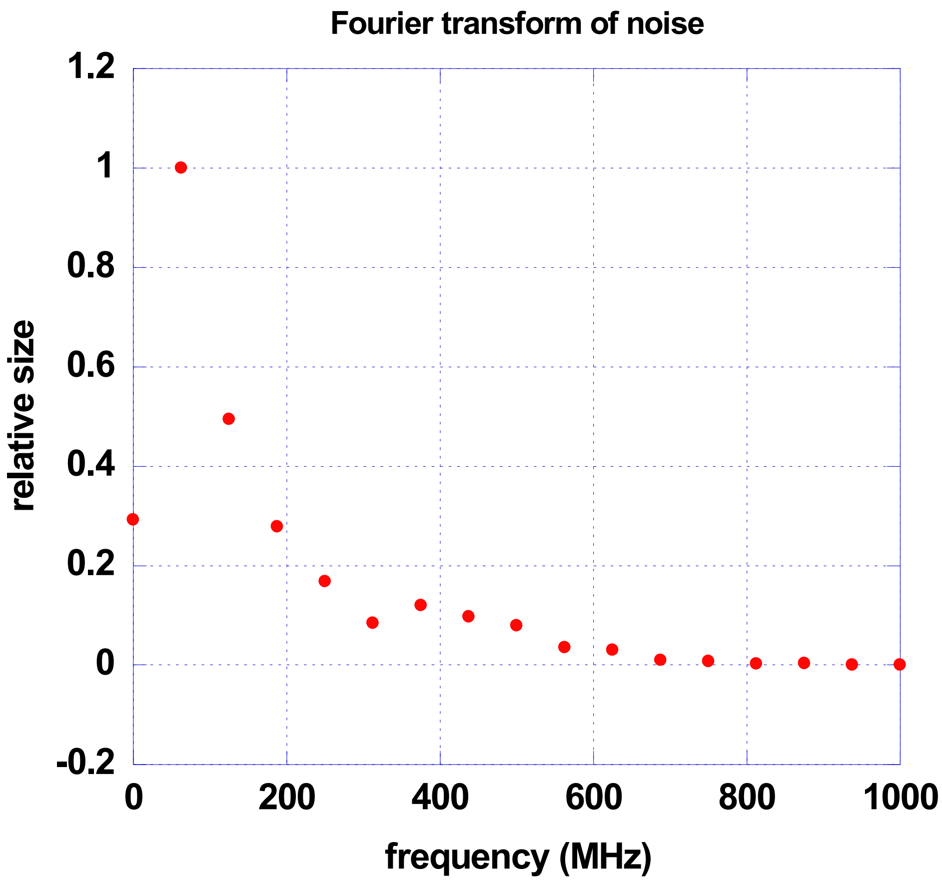

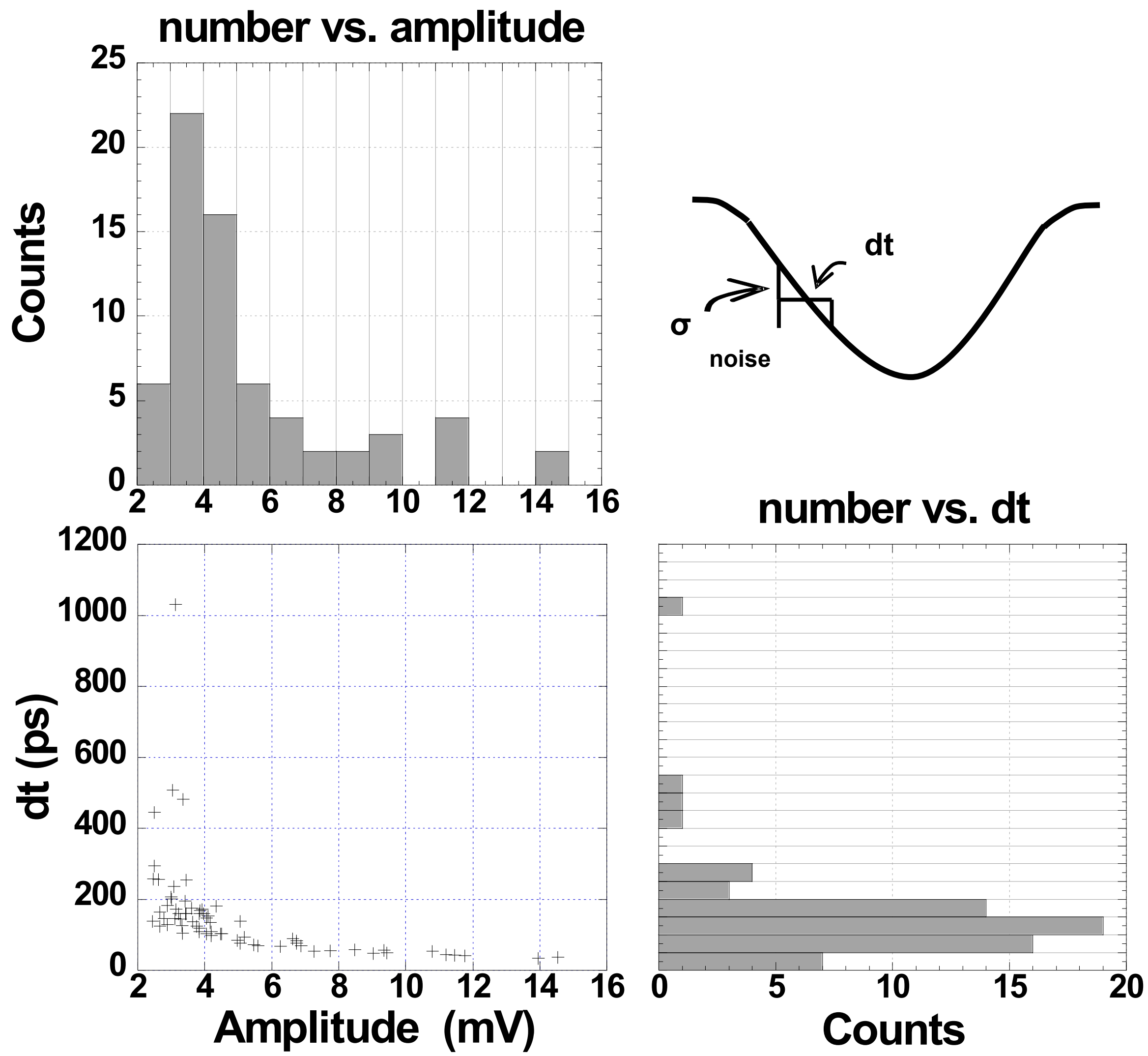

Scatter plot of expected noise-induced timing errors, *dt*, vs. pulse amplitude, for 67 pulses and the projections of *dt* and amplitude distributions. σ (noise) = 0.33 mV.

1. **introduction**
2. **history**
3. **factors affecting speed**
4. **generating the signal – Ramo’s theorem**
5. **amplifying the signal – charge and current amplifiers**
6. **trench electrode sensors**
7. **hex-cell sensors**
8. **experimental results**
9. **analysis – constant fraction discrimination**
10. **analysis – fitting with almost-noise-free pulses**
11. **next**

1. **The approximately noise-free signal pulse shape from the digital oscilloscope shown earlier was scaled from small to large pulse heights.**
2. **A set of noise sequences was prepared from the pre-pulse base lines.**
3. **Each noise sequence was added, point-by-point, to the scaled-amplitude signal.**
4. **The scaled noise-free pulse was adjusted to have the same peak height as the pulse in 3, and the standard deviation of the point-by-point differences found as the relative timing of the two pulses was shifted point (62.5 ps) by point.**
5. **A parabola was fit to the minimum value of the standard deviation and the two values on each side, and its minimum used as the best-fit time.**
6. **This was repeated for each pulse height.**

Standard Deviation

$$\sqrt{\frac{\sum_{i=1}^{n} x_i^2 - n(\bar{x})^2}{n-1}}$$

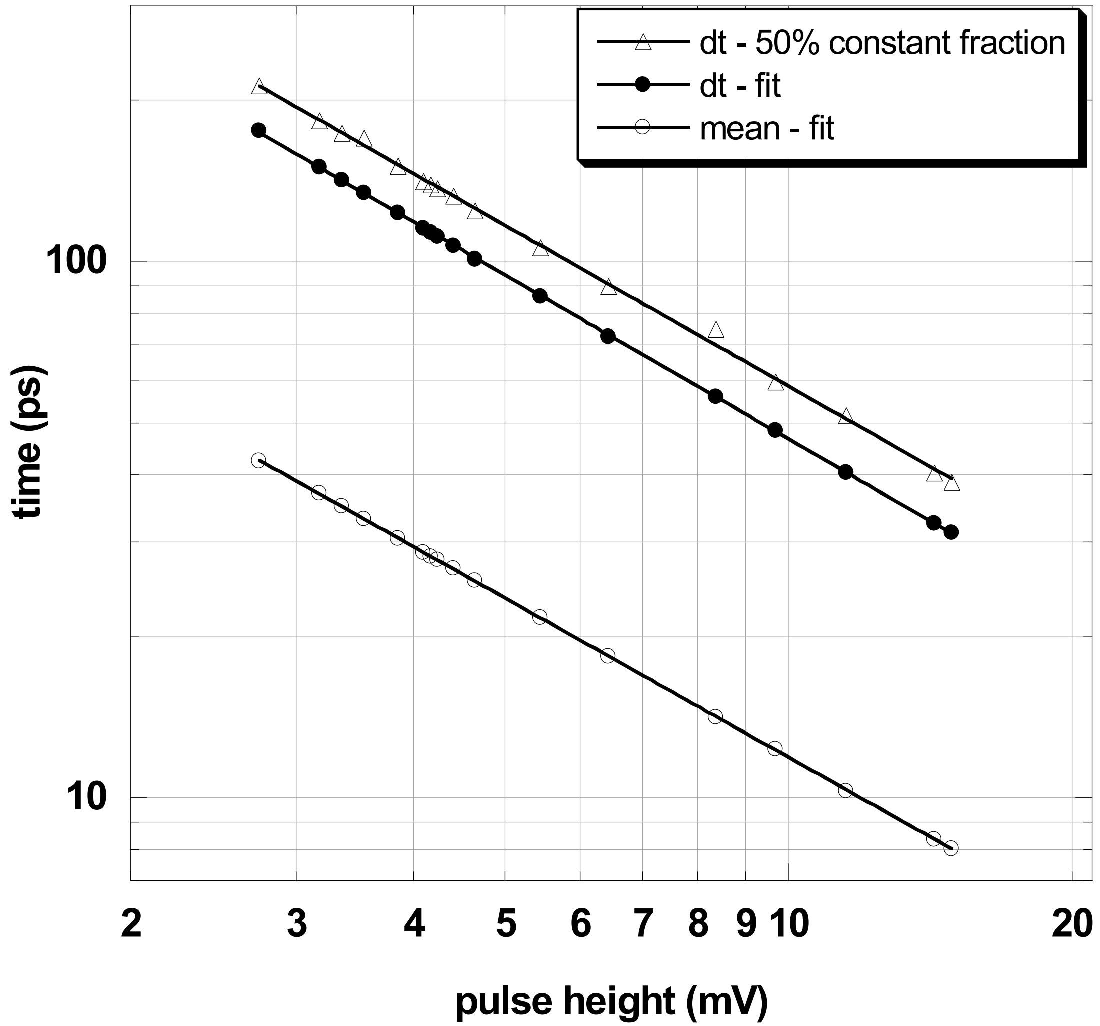

Expected time errors, dt, due to noise as a function of pulse height from the combined signal pulse shape added to 201 noise segments with dt determined from the standard deviation of time variation of the 50% point on the leading edge (Δ) and from the time variation of the best fit time of the combined signal pulse shape to the same shape plus noise (●). The mean value of the best fit times (○) is 24% of the fit values. The signal to noise ratio is 3 times the pulse height in mV.

1. **introduction**
2. **history**
3. **factors affecting speed**
4. **generating the signal – Ramo’s theorem**
5. **amplifying the signal – charge and current amplifiers**
6. **trench electrode sensors**
7. **hex-cell sensors**
8. **experimental results**
9. **analysis – constant fraction discrimination**
10. **analysis – fitting with almost-noise-free pulses**
11. **next**

NEXT

1. Reduce as far as practicable, the sensor capacitance.
2. Use reduced temperatures to reduce noise and double speeds.
3. Use an amplifier with the lowest possible noise, given the available space, heat removal capabilities, and speed requirements.
4. Use higher electric fields giving drift velocities ≈ saturation values.
5. Use trench-electrode sensors.
6. Use waveform recorders if a channel can fit within the area of a pixel. Only the large-amplitude part of the signal is needed. The baseline average can be kept as a single, updated number in storage.
7. Use multiple timing layers of detectors, if allowed by Coulomb scattering, space, and cost considerations – some possibly rotated to help with tracking,
8. Use a weighting factor, as suggested by the time-resolution vs. pulse height results, to favor layers having high signal-to-noise ratios.
9. Considering 6-8 above, use high-resolution position-tracking layers. The most accurate timing will be done by a system, not by one sensor – readout unit.

Some Partial Conclusions

- **With the latest 3D results we have seen a decrease in pulse times by 3 orders of magnitude.**
- **There should be possibilities of silicon sensor systems with time resolution well below 100 ps.**
- **The lowest times will use some combination of multiple layers, lower capacitances, higher voltages than the 20V we used, 1/amplitude weighting, lower temperatures, and/or improved electronics.**
- **Improved, fast, compact, wave-form digitizers could help.**
- **We can expect generic electronics certainly will also be improved by industry.**